First Results from the Planck satellite

A satellite to measure the Universe

F.-X. Désert
IPAG: Institut de Planétologie et d'Astrophysique de Grenoble
and LPSC + Institut Néel-MCBT

The Mission Makers

- ESA
- Thales Alenia Space, Air liquide
- CNES & CNRS (HFI)
- ASI (LFI)
- NASA
- CEA, Universities
- 13 laboratories (5 in France) in Europe & North America

www.planck.fr

www.rssd.esa.int/index.php?project=PLANCK&page=index

The Planckian People

The Scientists

29 laboratories

Planck Early Results: The *Planck* mission

Planck Collaboration: P. A. R. Ade[78], N. Aghanim[51], M. Arnaud[64], M. Ashdown[62,87], J. Aumont[51], C. Baccigalupi[76], M. Baker[35], A. Balbi[29], A. J. Banday[85,8,69], R. B. Barreiro[58], J. G. Bartlett[3,60], E. Battaner[89], K. Benabed[52], K. Bennett[36], A. Benoît[52], J.-P. Bernard[85,8], M. Bersanelli[27,44], R. Bhatia[36], J. J. Bock[60,9], A. Bonaldi[40], J. R. Bond[5], J. Borrill[68,80], F. R. Bouchet[52], T. Bradshaw[75], M. Bremer[36], M. Bucher[3], C. Burigana[43], R. C. Butler[43], P. Cabella[29], C. M. Cantalupo[68], B. Cappellini[44], J.-F. Cardoso[65,3,52], R. Carr[33], M. Casale[33], A. Catalano[3,63], L. Cayón[20], A. Challinor[88,62,11], A. Chamballu[49], J. Charra[51], R.-R. Chary[50], L.-Y Chiang[55], C. Chiang[19], P. R. Christensen[72,30], D. L. Clements[49], S. Colombi[52], F. Couchot[67], A. Coulais[63], B. P. Crill[60,73], G. Crone[36], M. Crook[75], F. Cuttaia[43], L. Danese[76], O. D'Arcangelo[59], R. D. Davies[61], R. J. Davis[61], P. de Bernardis[26], J. de Bruin[35], G. de Gasperis[29], A. de Rosa[43], G. de Zotti[40,76], J. Delabrouille[3], J.-M. Delouis[52], F.-X. Désert[47], J. Dick[76], C. Dickinson[61], K. Dolag[69], H. Dole[51], S. Donzelli[44,56], O. Doré[60,9], U. Dörl[69], M. Douspis[51], X. Dupac[34], G. Efstathiou[88], T. A. Enßlin[69], H. K. Eriksen[56], F. Finelli[43], S. Foley[35], O. Forni[85,8], P. Fosalba[53], M. Frailis[42], E. Franceschi[43], M. Freschi[34], T. C. Gaier[60], S. Galeotta[42], J. Gallegos[34], B. Gandolfo[35], K. Ganga[3,50], M. Giard[85,8], G. Giardino[36], Y. Giraud-Héraud[3], J. González[33], J. González-Nuevo[76], K. M. Górski[60,91], S. Gratton[62,88], A. Gregorio[28], A. Gruppuso[43], G. Guyot[46], J. Haissinski[67], F. K. Hansen[56], D. Harrison[88,62], G. Helou[9], S. Henrot-Versillé[67], C. Hernández-Monteagudo[69], D. Herranz[58], S. R. Hildebrandt[9,66,57], E. Hivon[52], M. Hobson[87], W. A. Holmes[60], A. Hornstrup[13], W. Hovest[69], R. J. Hoyland[57], K. M. Huffenberger[90], A. H. Jaffe[49], T. Jagemann[34], W. C. Jones[19], J. J. Juillet[83], M. Juvela[18], P. Kangaslahti[60], E. Keihänen[18], R. Keskitalo[60,18], T. S. Kisner[68], R. Kneissl[32,4], L. Knox[22], M. Krassenburg[36], H. Kurki-Suonio[18,38], G. Lagache[51], A. Lähteenmäki[1,38], J.-M. Lamarre[63], A. E. Lange[50], A. Lasenby[87,62], R. J. Laureijs[36], C. R. Lawrence[60], S. Leach[76], J. P. Leahy[61], R. Leonardi[34,36,23], C. Leroy[51,85,8], P. B. Lilje[56,10], M. Linden-Vørnle[13], M. López-Caniego[58], S. Lowe[61], P. M. Lubin[23], J. F. Macías-Pérez[66], T. Maciaszek[6], C. J. MacTavish[62], B. Maffei[61], D. Maino[27,44], N. Mandolesi[43], R. Mann[77], M. Maris[42], E. Martínez-González[58], S. Masi[26], M. Massardi[40], S. Matarrese[25], F. Matthai[69], P. Mazzotta[29], A. McDonald[35], P. McGehee[50], P. R. Meinhold[23], A. Melchiorri[26], J.-B. Melin[12], L. Mendes[34], A. Mennella[27,42], C. Mevi[35], R. Miniscalco[35], S. Mitra[60], M.-A. Miville-Deschênes[51,5], A. Moneti[52], L. Montier[85,8], G. Morgante[43], N. Morisset[48], D. Mortlock[49], D. Munshi[78,88], A. Murphy[71], P. Naselsky[72,30], P. Natoli[29,2,43], C. B. Netterfield[15], H. U. Nørgaard-Nielsen[13], F. Noviello[51], D. Novikov[49], I. Novikov[72], I. J. O'Dwyer[60], I. Ortiz[33], S. Osborne[82], P. Osuna[33], C. A. Oxborrow[13], F. Pajot[51], R. Paladini[81,9], B. Partridge[37], F. Pasian[42], T. Passvogel[36], G. Patanchon[3], D. Pearson[60], T. J. Pearson[9,50], O. Perdereau[67], L. Perotto[66], F. Perrotta[76], F. Piacentini[26], M. Piat[3], E. Pierpaoli[17], S. Plaszczynski[67], P. Platania[59], E. Pointecouteau[85,8], G. Polenta[2,41], N. Ponthieu[51], L. Popa[54], T. Poutanen[38,18,1], G. Prézeau[9,60], S. Prunet[52], J.-L. Puget[51], J. P. Rachen[69], W. T. Reach[86], R. Rebolo[57,31], M. Reinecke[69], J.-M. Reix[83], C. Renault[66], S. Ricciardi[43], T. Riller[69], I. Ristorcelli[85,8], G. Rocha[60,9], C. Rosset[3], M. Rowan-Robinson[49], J. A. Rubiño-Martín[57,31], B. Rusholme[50], E. Salerno[7], M. Sandri[43], D. Santos[66], G. Savini[74], B. M. Schaefer[84], D. Scott[16], M. D. Seiffert[60,9], P. Shellard[11], A. Simonetto[59], G. F. Smoot[21,68,3], C. Sozzi[59], J.-L. Starck[64,12], J. Sternberg[36], F. Stivoli[45], V. Stolyarov[87], R. Stompor[3], L. Stringhetti[43], R. Sudiwala[78], R. Sunyaev[69,79], J.-F. Sygnet[52], D. Tapiador[33], J. A. Tauber[36] *, D. Tavagnacco[42], D. Taylor[33], L. Terenzi[43], D. Texier[33], L. Toffolatti[14], M. Tomasi[27,44], J.-P. Torre[51], M. Tristram[67], J. Tuovinen[70], M. Türler[48], G. Umana[39], L. Valenziano[43], J. Valiviita[56], J. Varis[70], L. Vibert[51], P. Vielva[58], F. Villa[43], N. Vittorio[29], L. A. Wade[60], B. D. Wandelt[52,24], C. Watson[35], S. D. M. White[69], M. White[21], A. Wilkinson[61], D. Yvon[12], A. Zacchei[42], and A. Zonca[23]

[astro-ph.IM] 11 Jan 2011

Jan 2011: 25 papers submitted to an A&A special issue

Planck in a nutshell

- Third generation satellite for the 3K CMB measurement, after COBE and WMAP
- 1900 kg at take-off (Ariane 5, 14 may 2009), small halo orbit around Lagrange point L2
- Off-axis Gregorian telescope: primary 1.5m, secondary 1m, main axis pointing at 85 degrees away from the spin axis.
- 2kW, Telemetry: 100kbit/s (3 hours download per day), 2TeraBytes per year
- Warm launch, passive cooling and complex cryogenic chain, with 2 cryo coolers (20 and 4 K), open-cycle dilution 1.6, 0.1K (48.000 litres of Helium)
- 52 bolometers (HFI) et 22 radiometers (LFI)
- >4 complete maps of the continuum sky at 9 frequencies: 30-900 GHz (1cm-0.33mm). Scanning at 1rpm.
- 600 scientists, 650 MEuros, 1991-2009, M-class ESA project (450 MEuros for ESA)
- HFI= 150 MEuros of which 56% France : CNES+CNRS

The short marriage

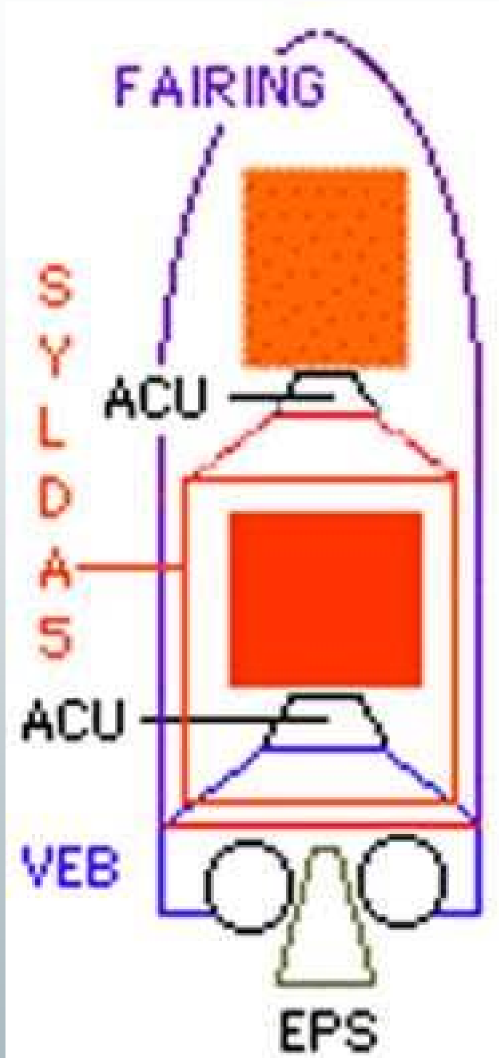

Sylda: Système de Lancement Double sur Ariane

Planck launch 14 May 2009

Launch (14 May 2009)

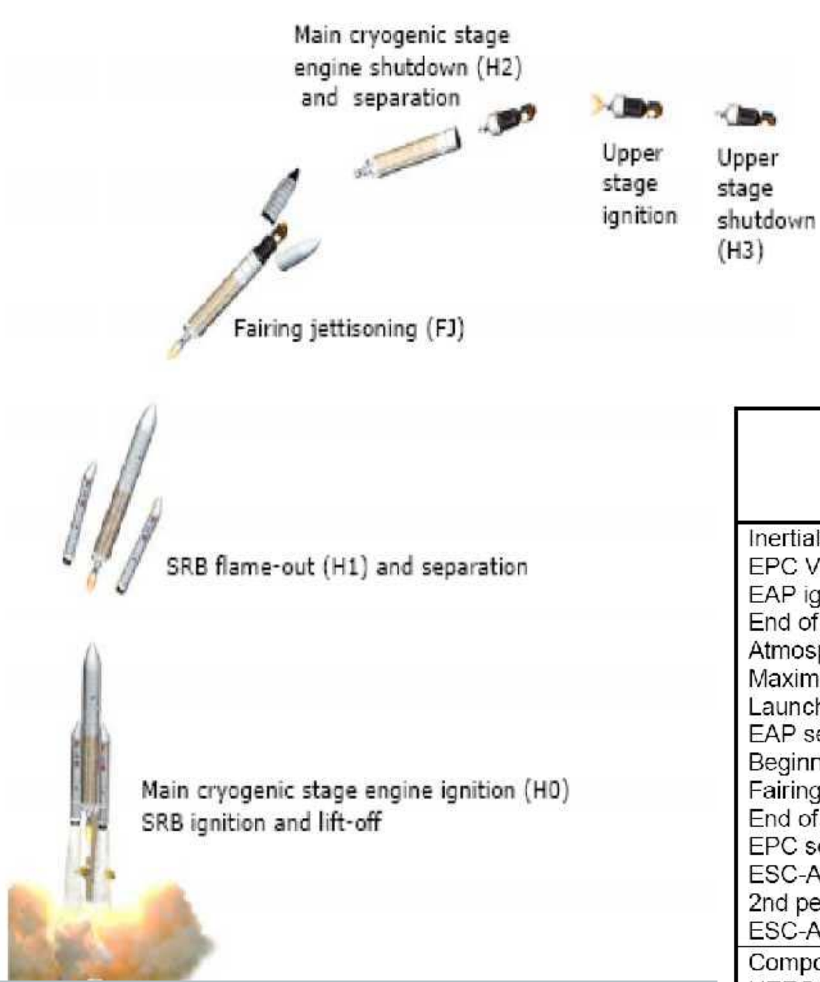

Ariane 5 ECA from Kourou, Guyanna
28th success, 44th launch
6 tons payload (inc. Sylda+ACU)
780 tons at H0
13 MNewton at takeoff

EVENT	COUNT	TIME (s) ALTITUDES A5-ECA RAMP results (Optimal case)	
Inertial platform release		- 3	0
EPC Vulcain engine ignition command	H0	0	
EAP ignition and Lift-Off		7.05	
End of vertical rise, beginning of pitch motion		12.05	
Atmospheric flight at zero angle of attack		25.32	
Maximum dynamic pressure		68.0	
Launch vehicle acceleration threshold detection	H1	139.78	65.84
EAP separation		140.56	
Beginning of guidance		145.86	
Fairing jettisoning		190.62	104.98
End of EPC main thrust phase	H2	536.63	
EPC separation		542.63	160.98
ESC-A Ignition		549.63	159.67
2nd peak of aeroflux		767.00	
ESC-A shutdown -Injection	H3	1495.35	968.44
Composite orientation to separation attitude		1508.25	
HERSCHEL separation	H4.1	1629.25	
Composite orientation		1639.05	
SYLDA-5 separation	H4.2	1789.35	
Composite reorientation		1799.75	
PLANCK separation	H4.3	1910.35	
ESC-A avoidance manoeuvres		1936.25	
End of launch vehicle mission		2507.05	

Cruise to L2

- After 1 day: 220 000 km, 2 days: 340 000 km
- HFI turned on for 2 days, after 5h, cryogenic opérations: cernox, dilution et 4K
- Commissionning: 48 days
  Non-contamination (170 K): 15 days
  Passive cooling and
  Cryogenics (reach L2 and 100mK): 33 days
- Calibration phase: 40 days
- 1st survey L+3 months (August 2009)
- One survey every 6 months

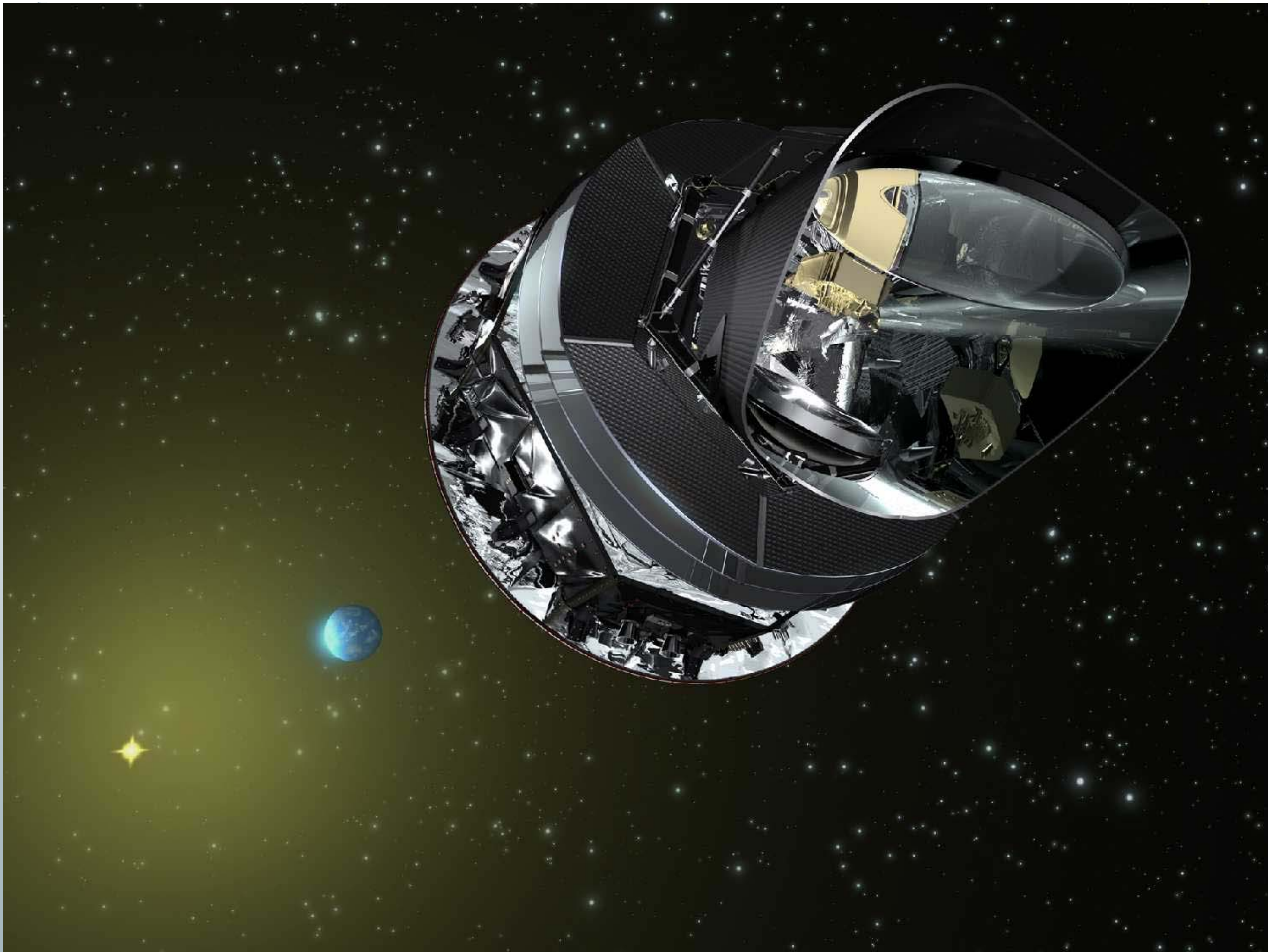

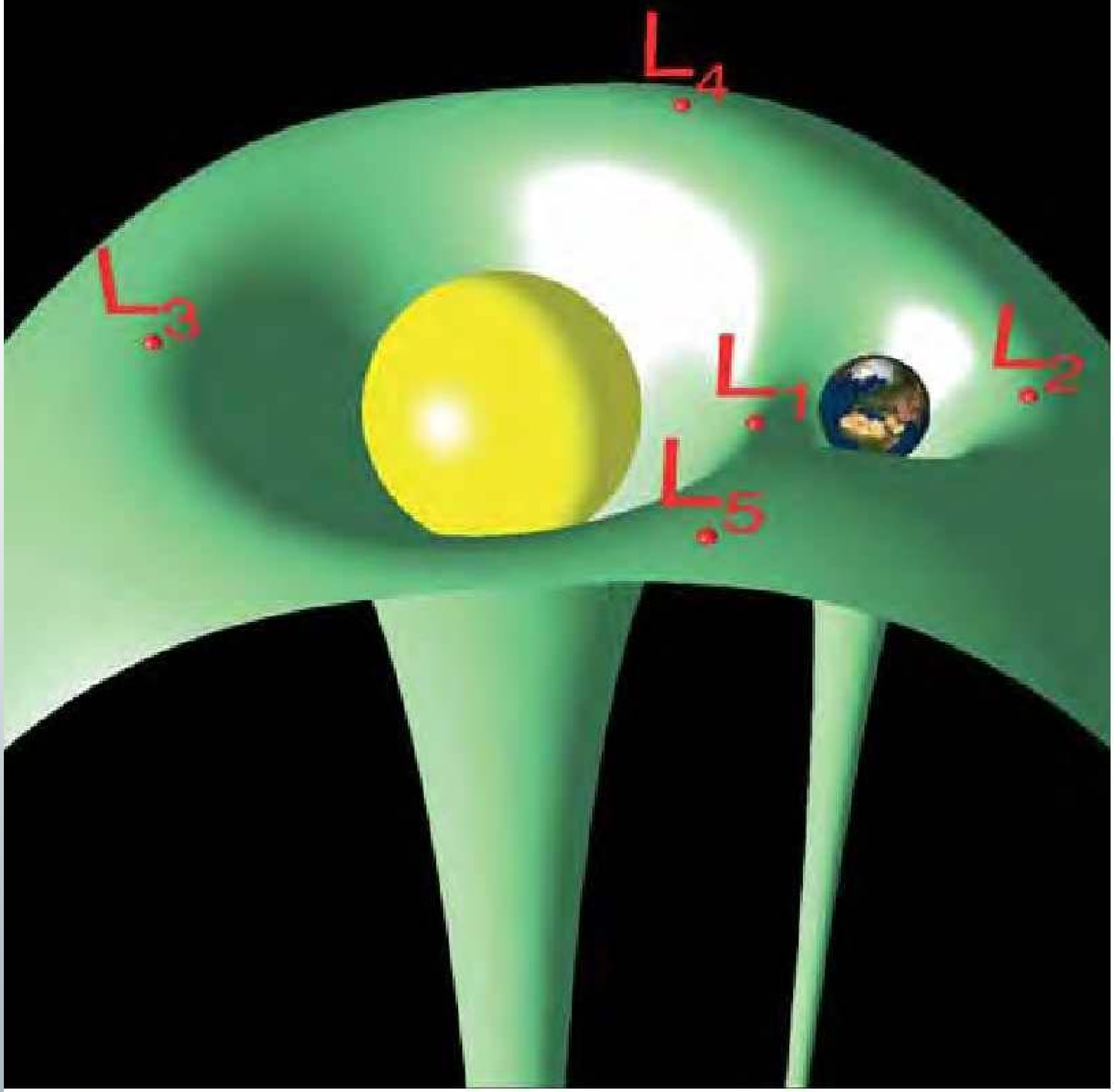

Lagrange (libration) points L1 to L5 on the 'Jacobi surface' (green) in the Sun-Earth system (not to scale)

Missions to L2
- WMAP
- Planck
- Herschel
- GAIA
- JWST
- Euclid?
- SPICA?
- Darwin?

À L1:
- Soho, ACE

Spin axis / AntiSolar <~ 10 deg.
Spin axis / Earth <~ 15 deg.

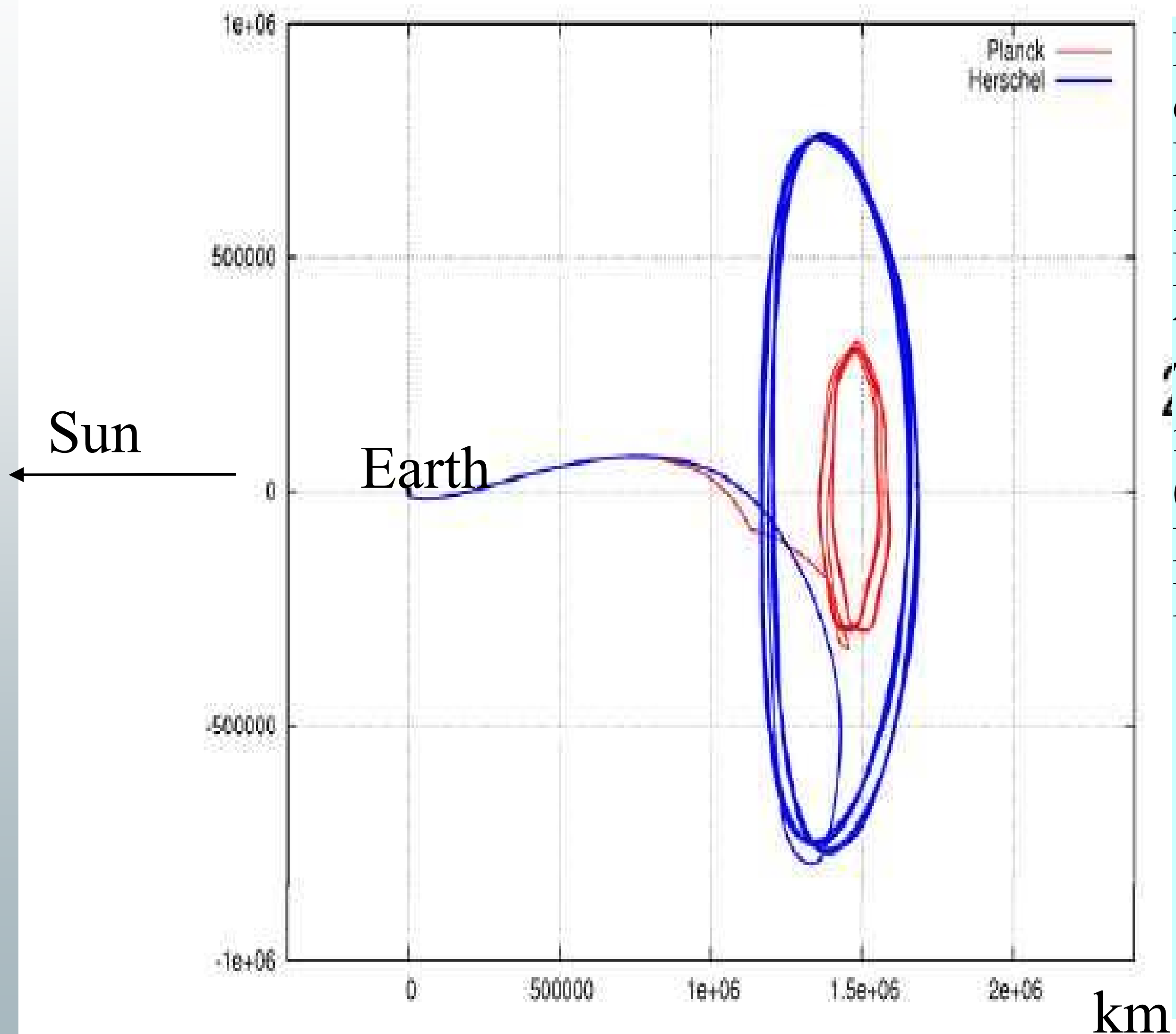

Lagrange points were discovered by Euler (3 coaligned ones) in 1750.
Lagrange established the 5 solutions.
The equilibrium point is unstable (23 days timescale).
Halo orbits and Lissajous orbits are stable.

Optics

The time machine

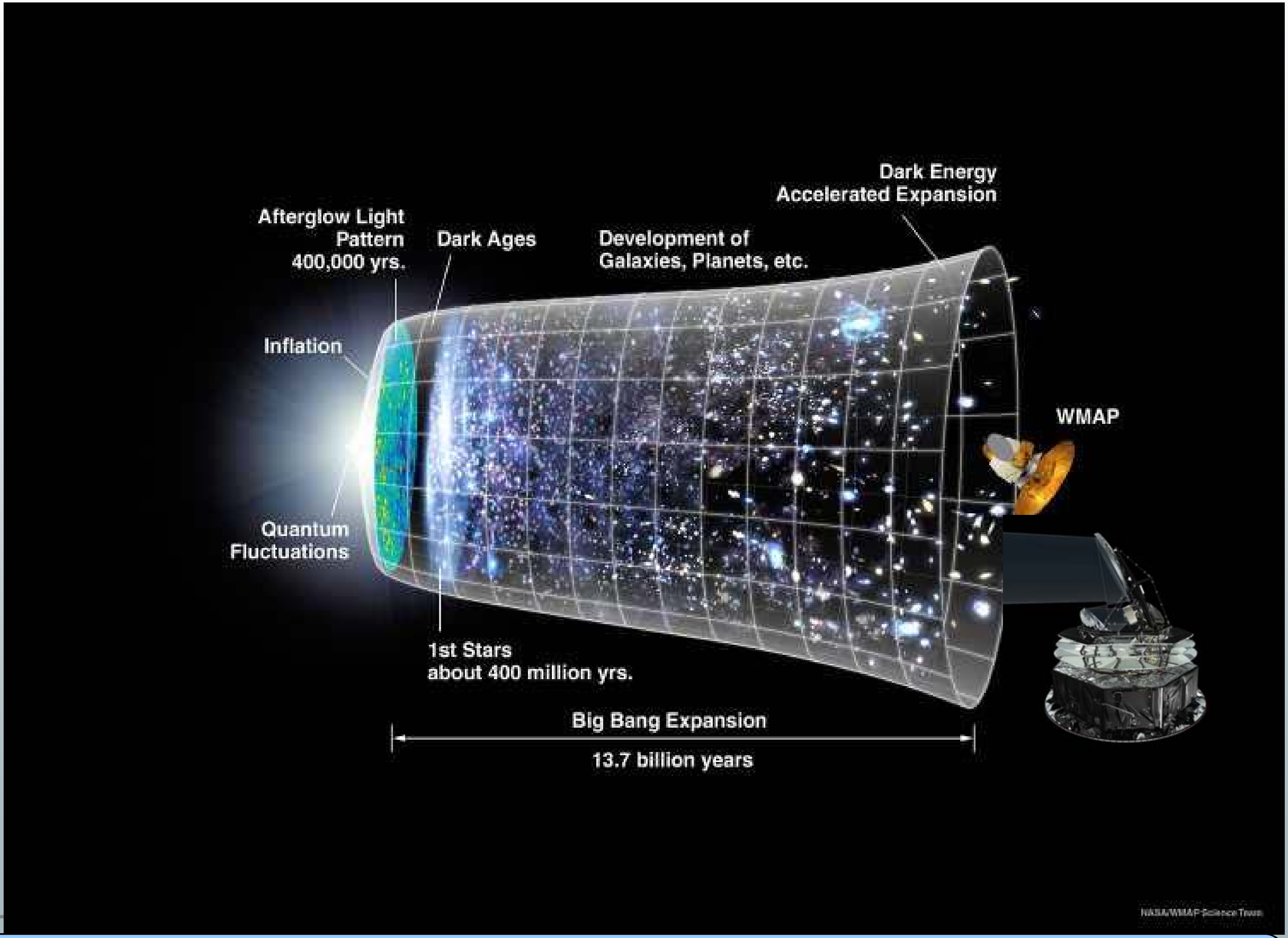

Map of the temperature fluctuations of the 3K CMB measured by WMAP. The tiny fluctuations are shown on an all sky Mollweide projection. Peak-to-peak variations of 0.02 % with respect to the mean temperature of 2.725 Kelvin. (NASA and WMAP Collaboration)

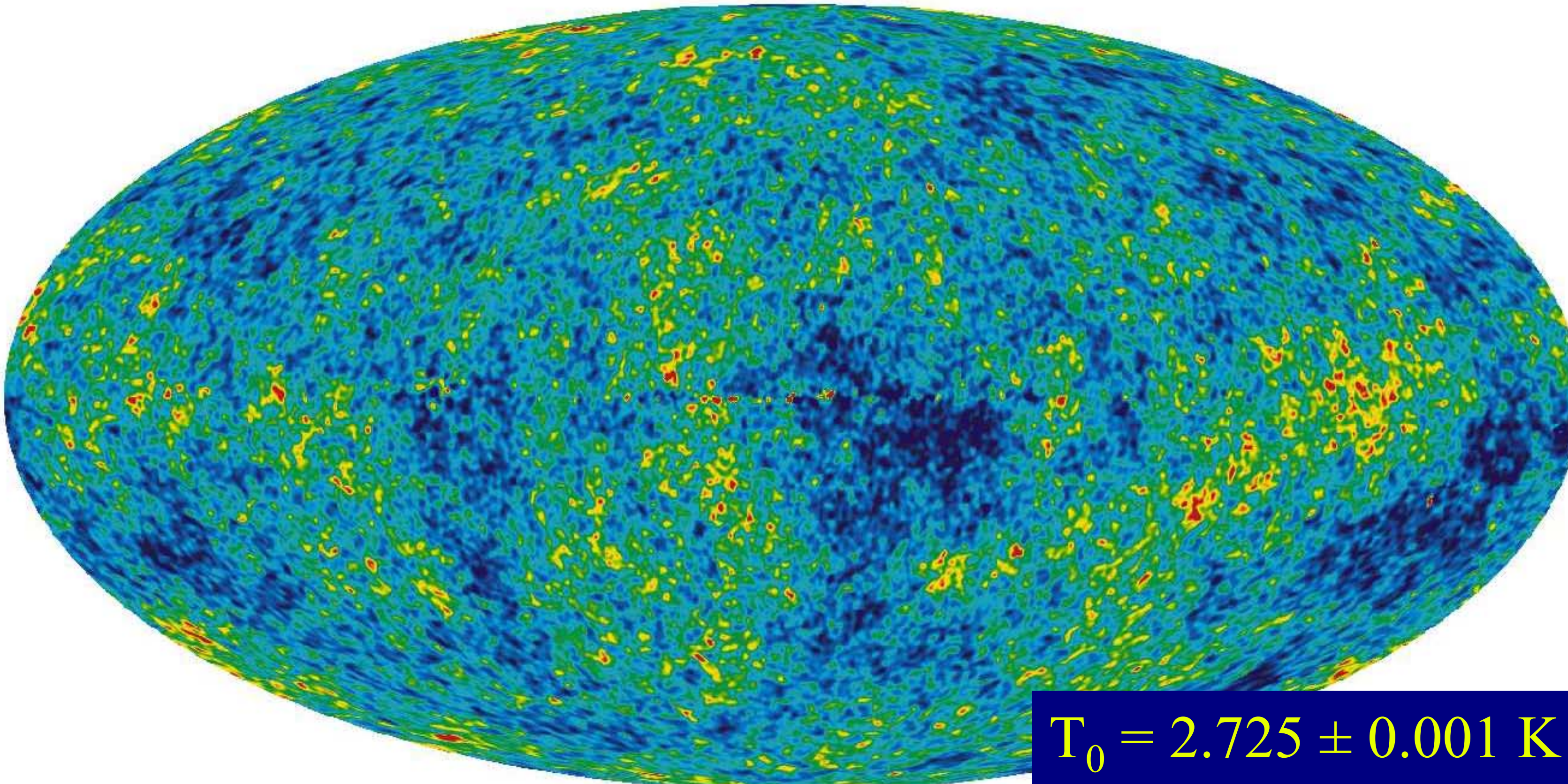

$T_0 = 2.725 \pm 0.001$ K (COBE

$\Delta T \sim 100\ \mu K$ (WMAP)

- Measure cosmological parameters
- Initial conditions leading to the formation of galaxies
- Constraints on the primordial universe and particle physics

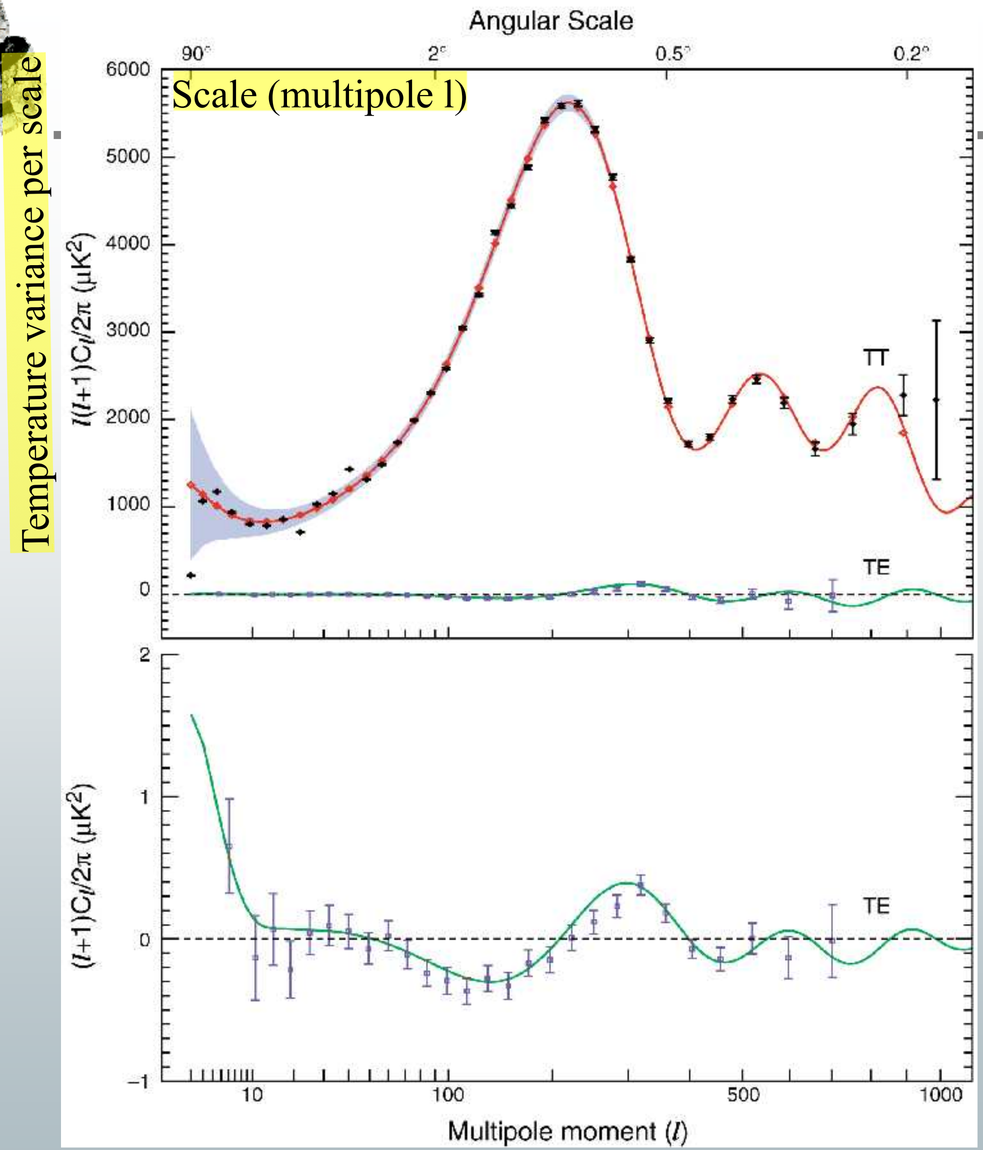

Hinshaw et al, 2006, astroph/0603451

$\Omega_{tot} = 0.99 \pm 0.02$

$\Omega_\Lambda = 0.75 \pm 0.04$

+SNLS

$w = -0.98 \pm 0.08$

$\Omega_m = 0.24 \pm 0.02$

$\Omega_b = 0.042 \pm 0.002$

$n_s = 0.95 \pm 0.02$

$\tau = 0.09 \pm 0.03$

$h = 0.73 \pm 0.03$

$\sigma_8 = 0.75 \pm 0.05$

WMAP + ACBAR + CBI + 2dF + Lyα

Spergel et al, 2006, astroph/0603449

WMAP 3 years TT & TE, χ^2/dof=1.04

Cosmological parameters

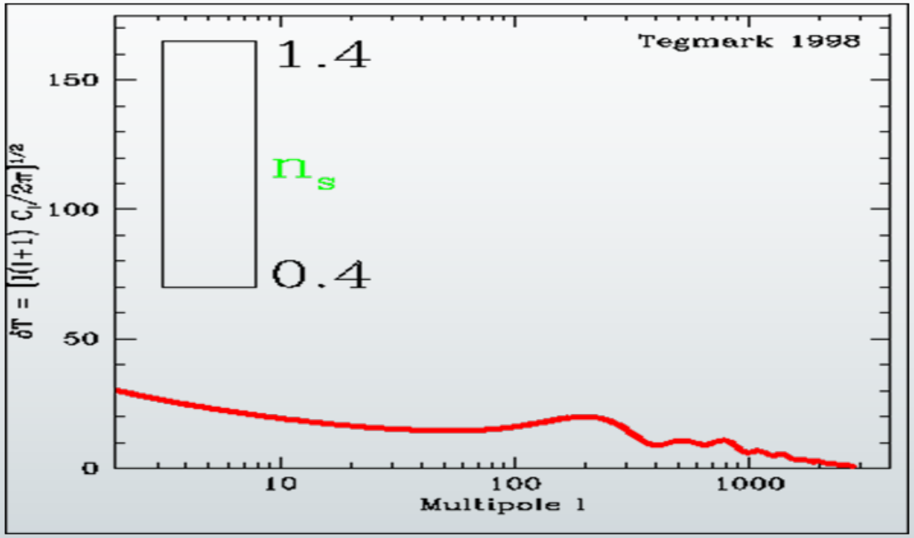

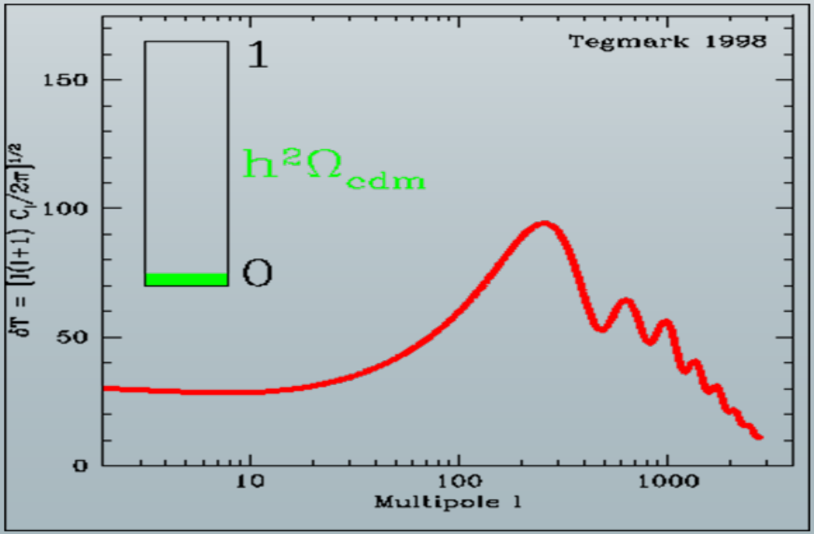

Parameter constraints

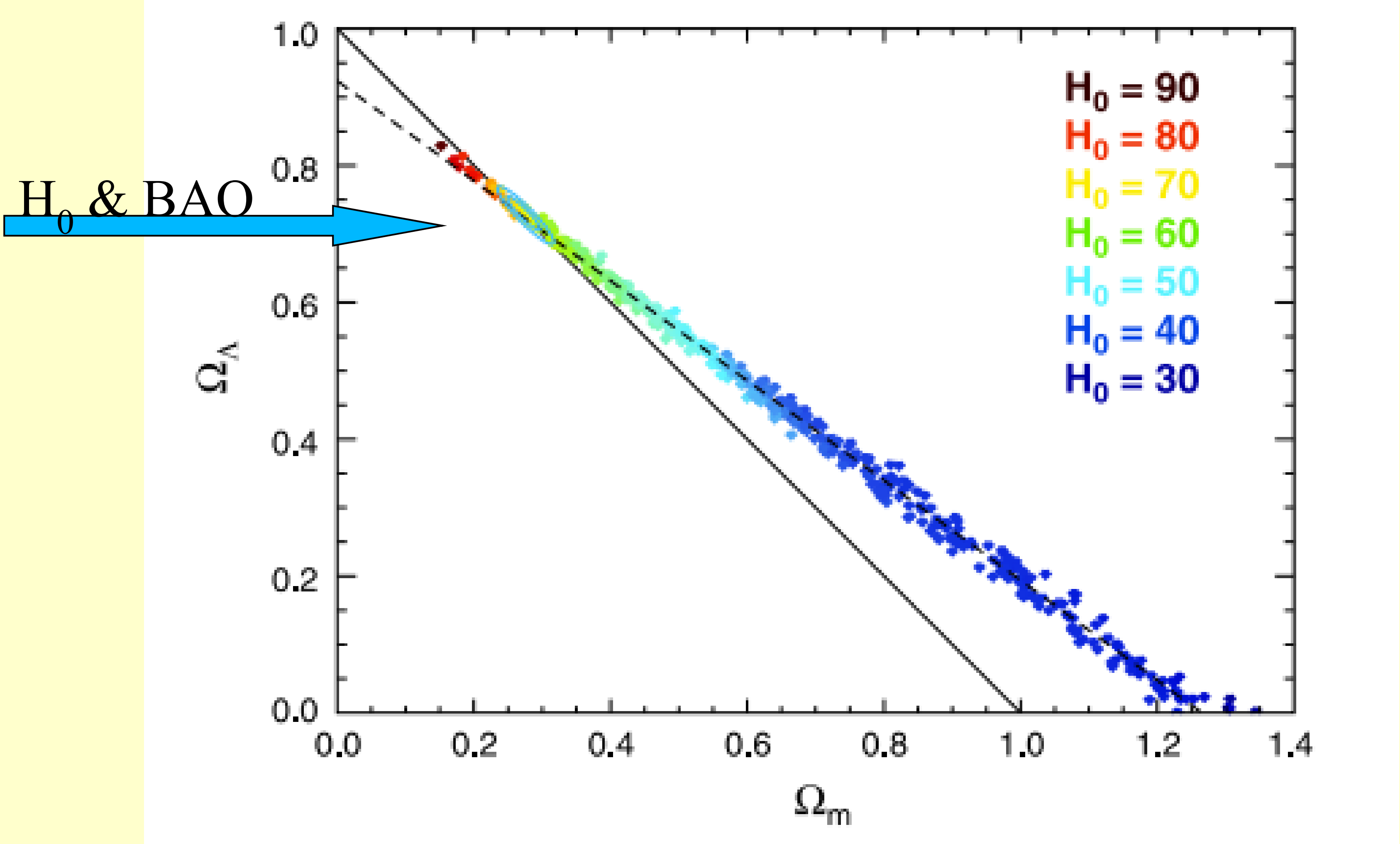

Larson et al. WMAP7yr 2010

Concordance model

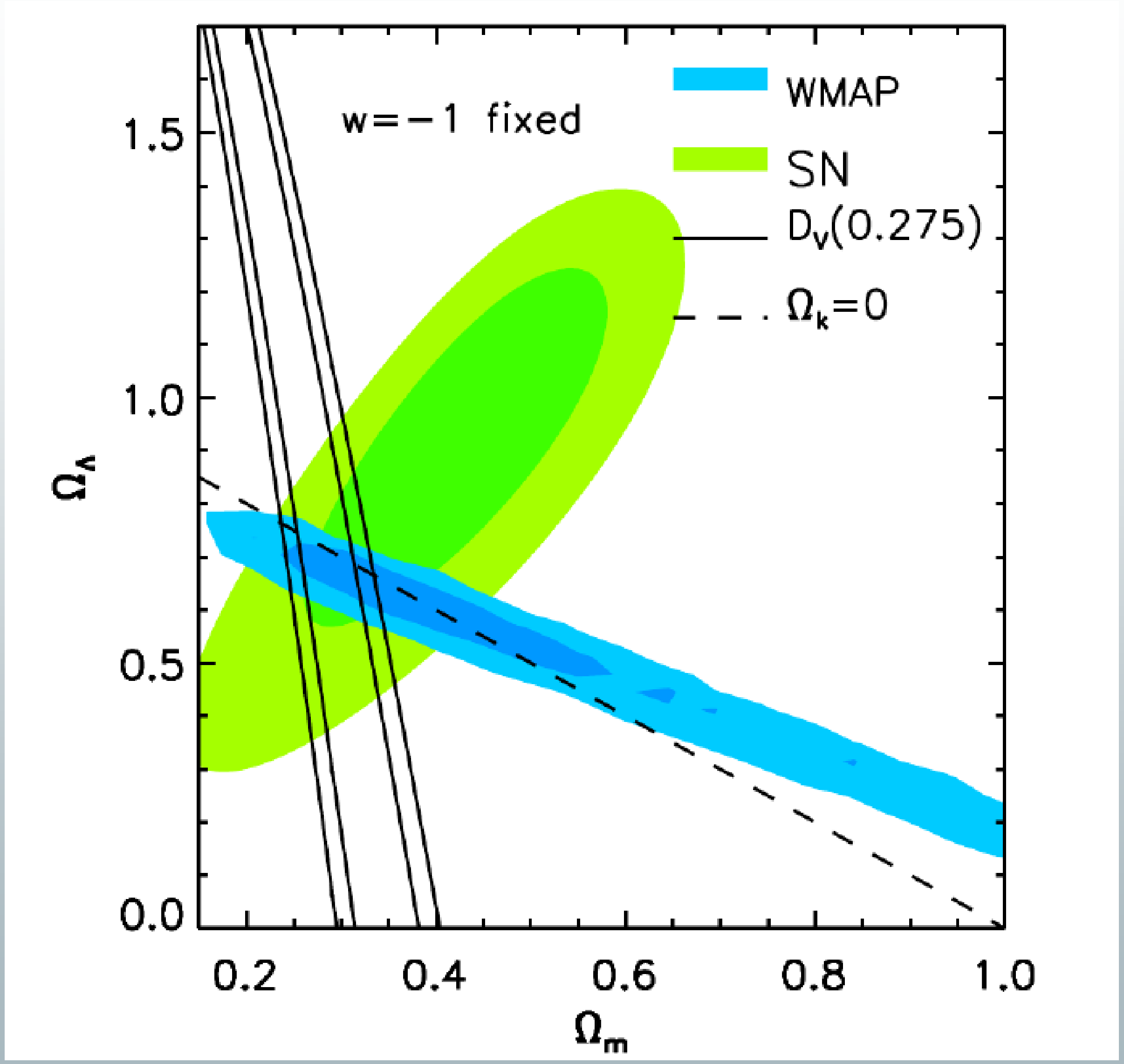

Dv = BAO constraint
Credits: Percival et coll., MNRAS, 2009, arXiv0907.1660

Our Strange Universe

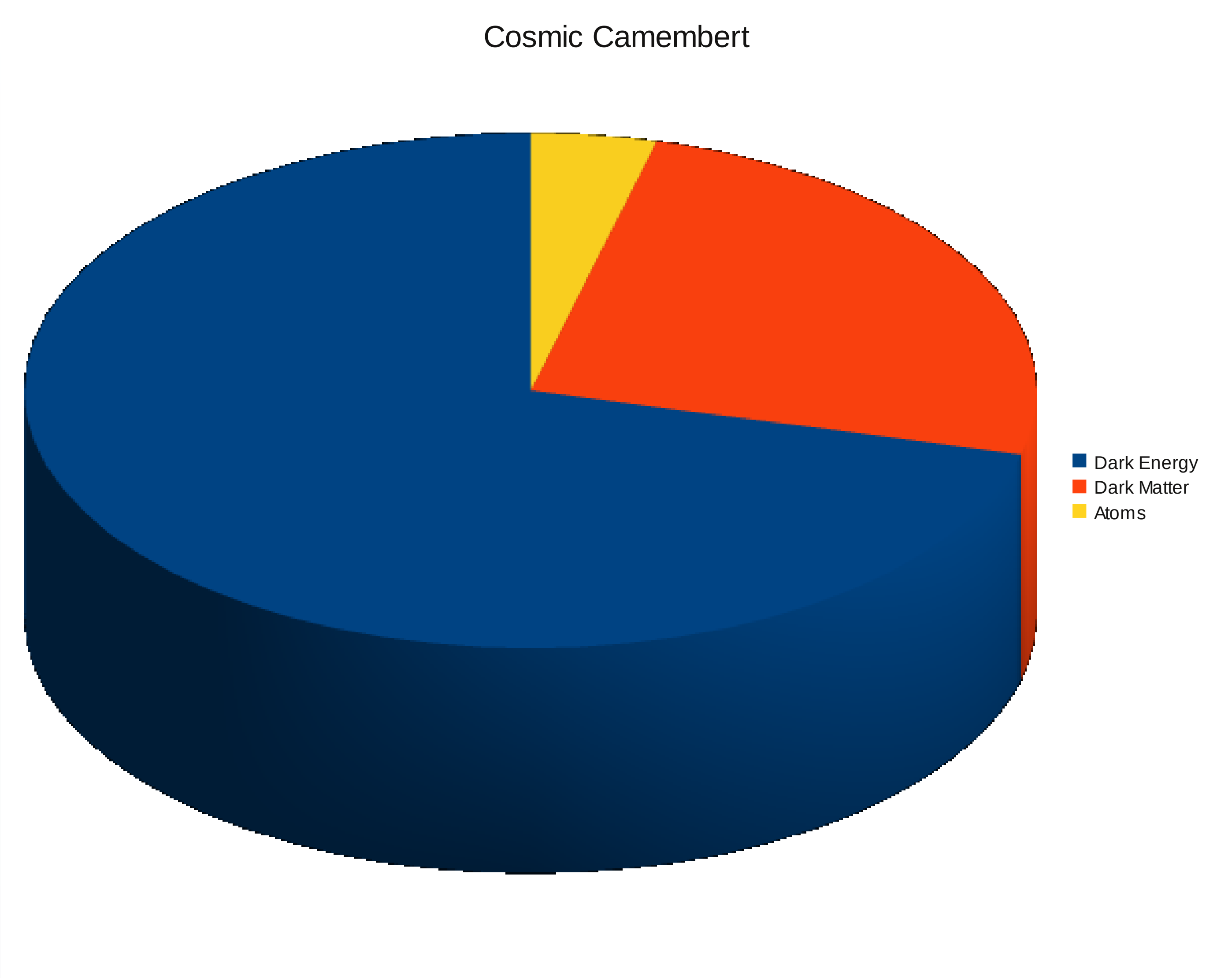

Planck: towards precision

Planck: Bolometers near the 3K CMB photon noise limit
In temperature,
limited by cosmic variance
(one sample of Universe)

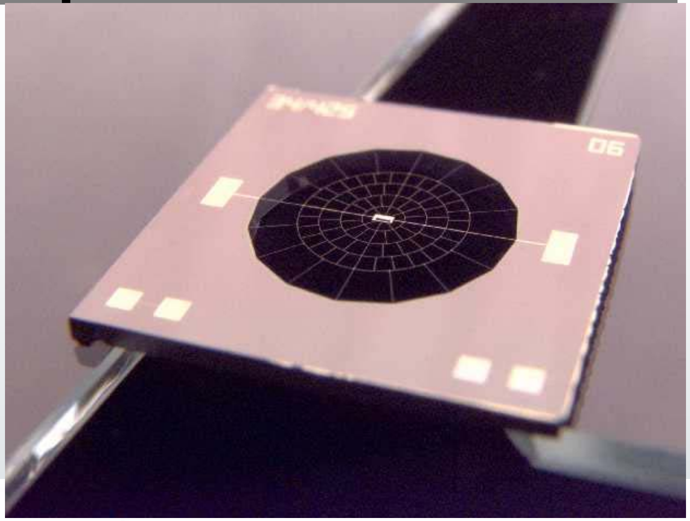

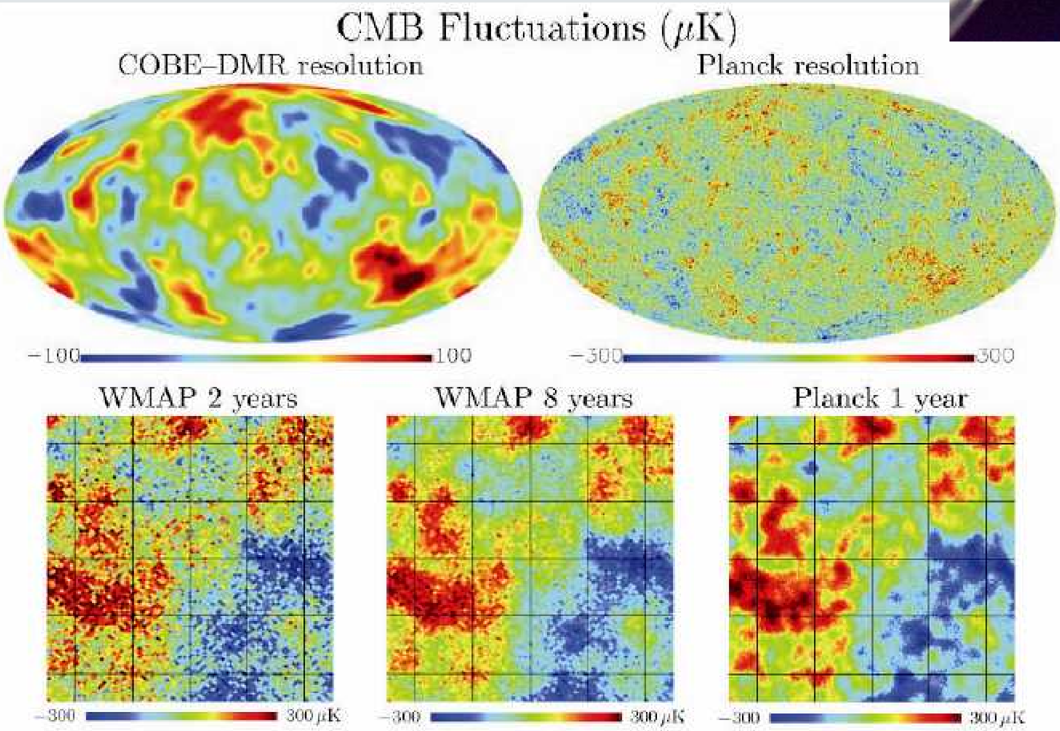

Cartes simulées du ciel CMB par le modèles cosmologique standart. Les 2 figures du haut montrent pour l'ensemble du ciel les anisotropies en température et les différences de résolution entre COBE (en haut à gauche) et Planck (en haut à droite). De même, les 3 figures du bas montrent les différences très significatives entre les résolutions WMAP (94 GHz, 15' FWHM, 2 ou 8 ans d'observation) et PLANCK (217 GHz, 5' FWHM, 1 an d'observation), calculées et cumulées au niveau « bruit de mesure ».

BlueBook

Planck: towards angular resolution

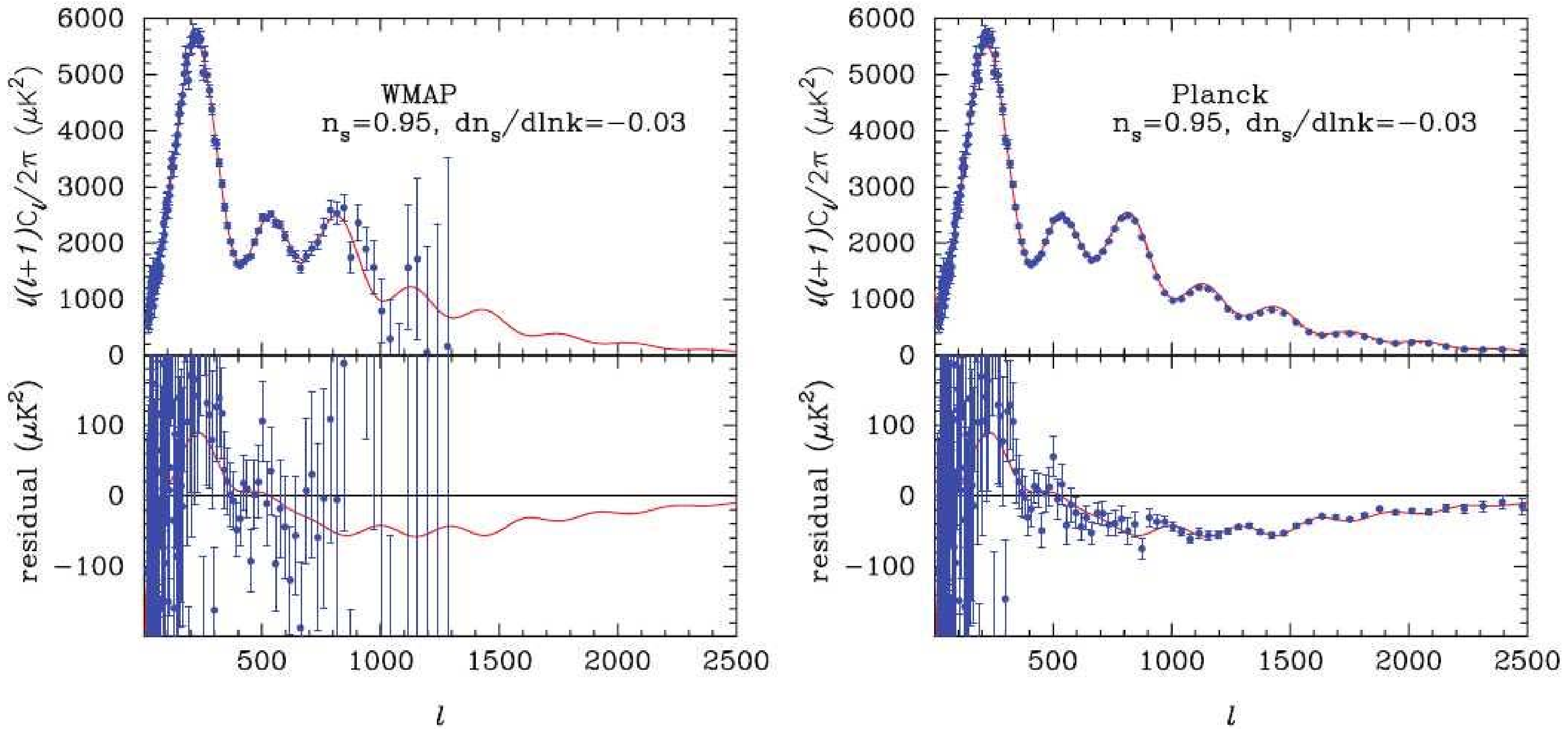

FIG 2.12.—Same as Figure 2.11, but now comparing the concordance ΛCDM model, having $n_S = 0.95$ and zero run (solid line), with a realisation of a model having with $n_S = 0.95$ (at a fiducial wavenumber of $k_0 = 0.05$ Mpc^{-1}) and a run of $dn_S/d\ln k = -0.03$.

BlueBook

Planck: towards polarization

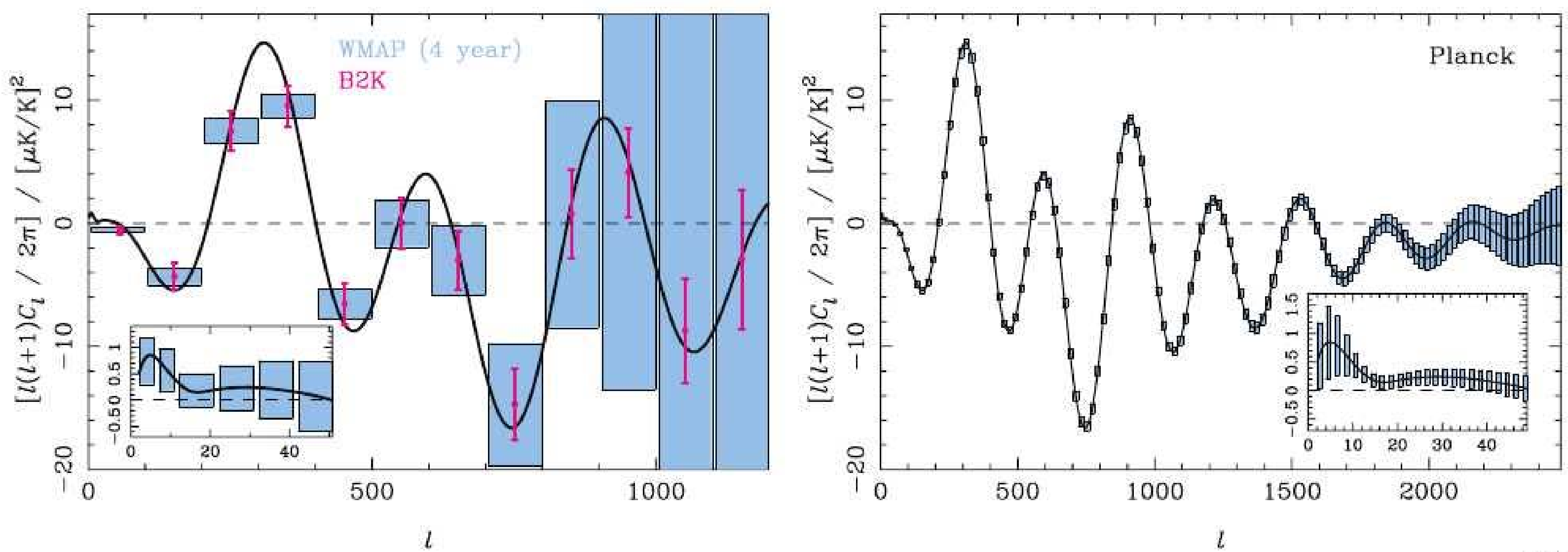

FIG 2.13.—Forecasts for the $\pm1\sigma$ errors on the temperature-polarization cross-correlation power spectrum C_ℓ^{TE} in a ΛCDM model (with $r = 0.1$ and $\tau = 0.17$) from *WMAP* (4 years of observation) and BOOMERanG2K (left) and *Planck* (right). In the left-hand plot, flat band powers are estimated with $\Delta\ell = 100$ for both experiments for ease of comparison. The inset shows the *WMAP* forecasts on large angular scales with a finer $\Delta\ell$ resolution. For *Planck*, flat band powers are estimated with $\Delta\ell = 20$ in the main plot, but with $\Delta\ell = 2$ in the inset on large scales.

BlueBook

Planck: towards our Universe

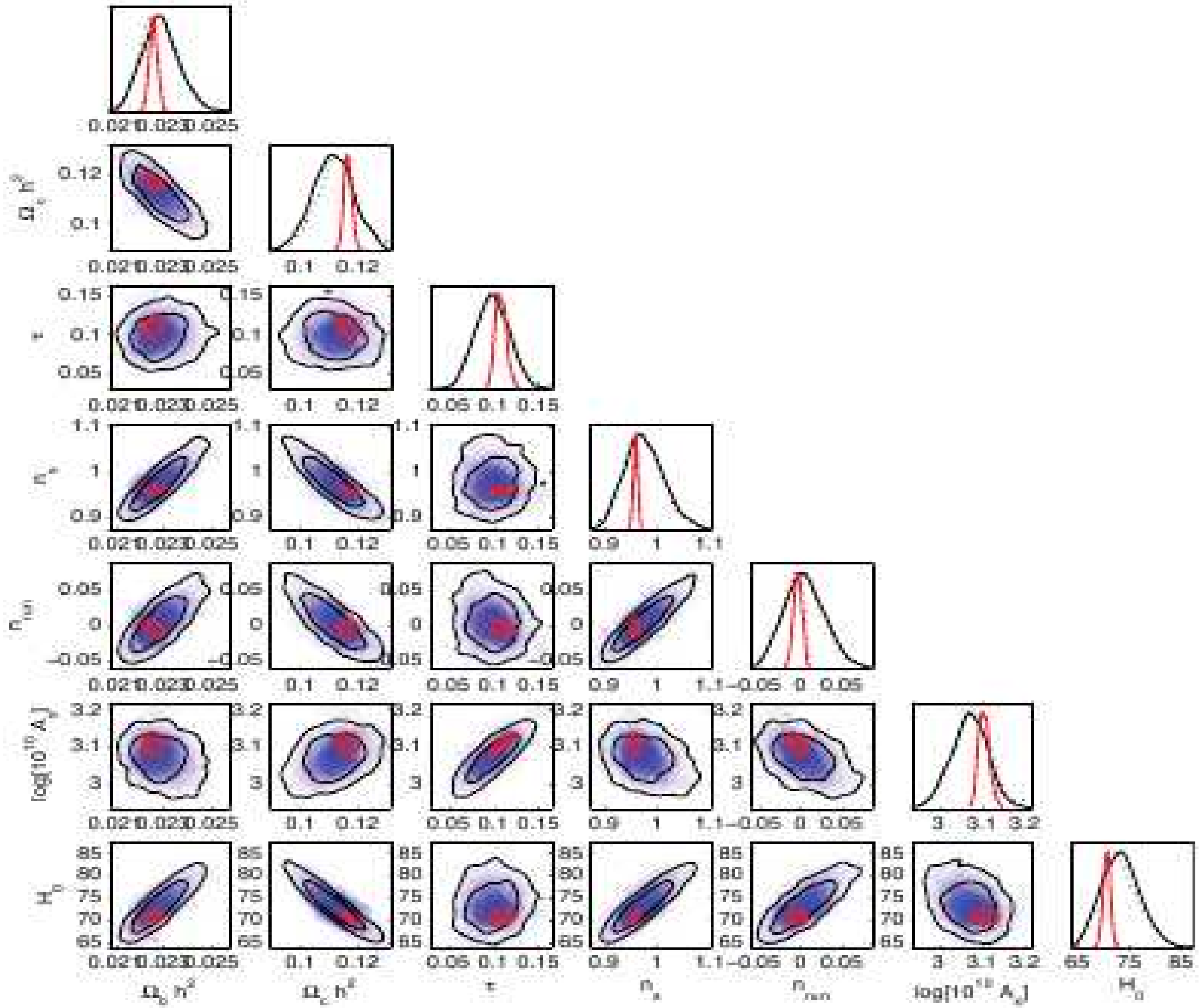

FIG. 2.18.—Forecasts of 1 and 2σ contour regions for various cosmological parameters when the spectral index is allowed to run. Blue contours show forecasts for *WMAP* after 4 years of observation and red contours show results for *Planck* after 1 year of observations. The curves show marginalized posterior distributions for each parameter.

The cryogenic chain

Sat + 20K + 4K + Dil + LFI + HFI

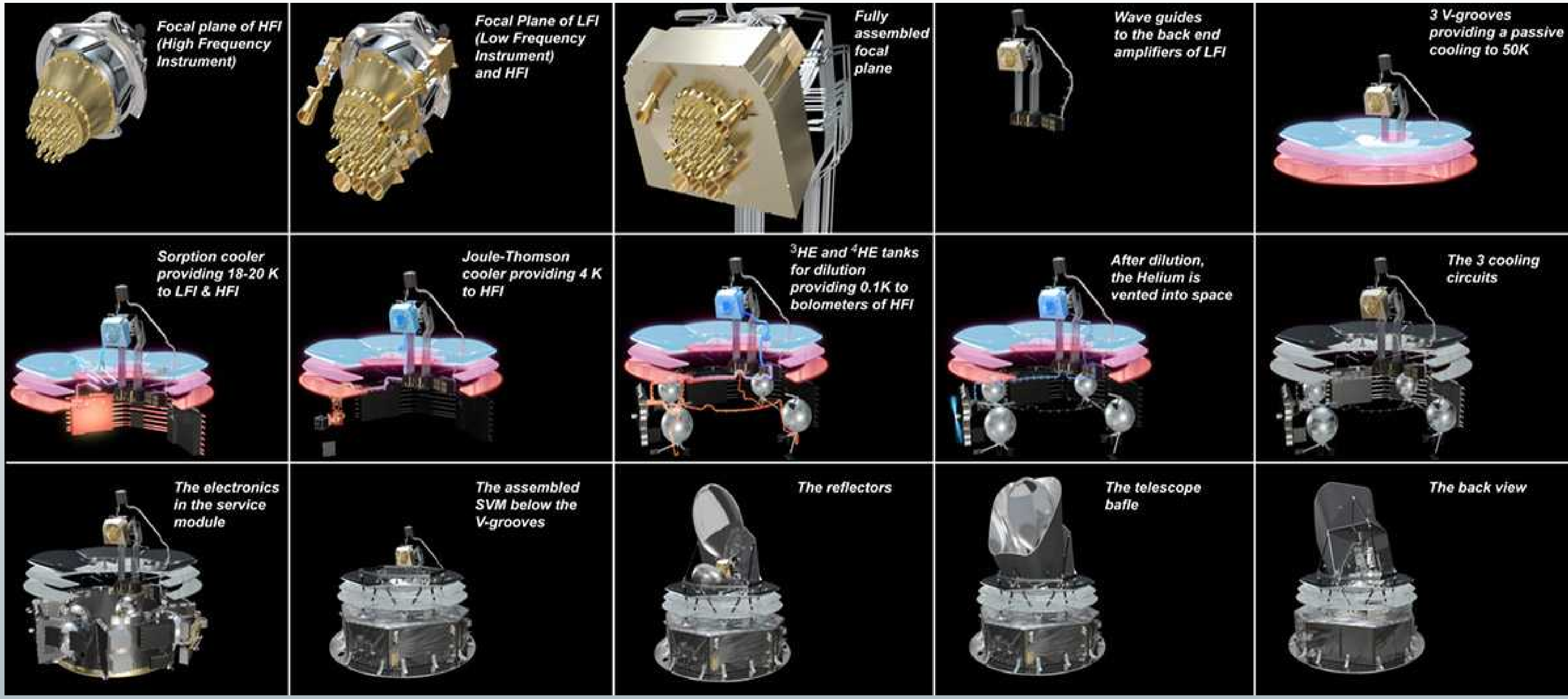

Incidents:4K, CR, Scanning,Transponder

Planck cooldown

Planck Collaboration: The thermal performance of *Planck*

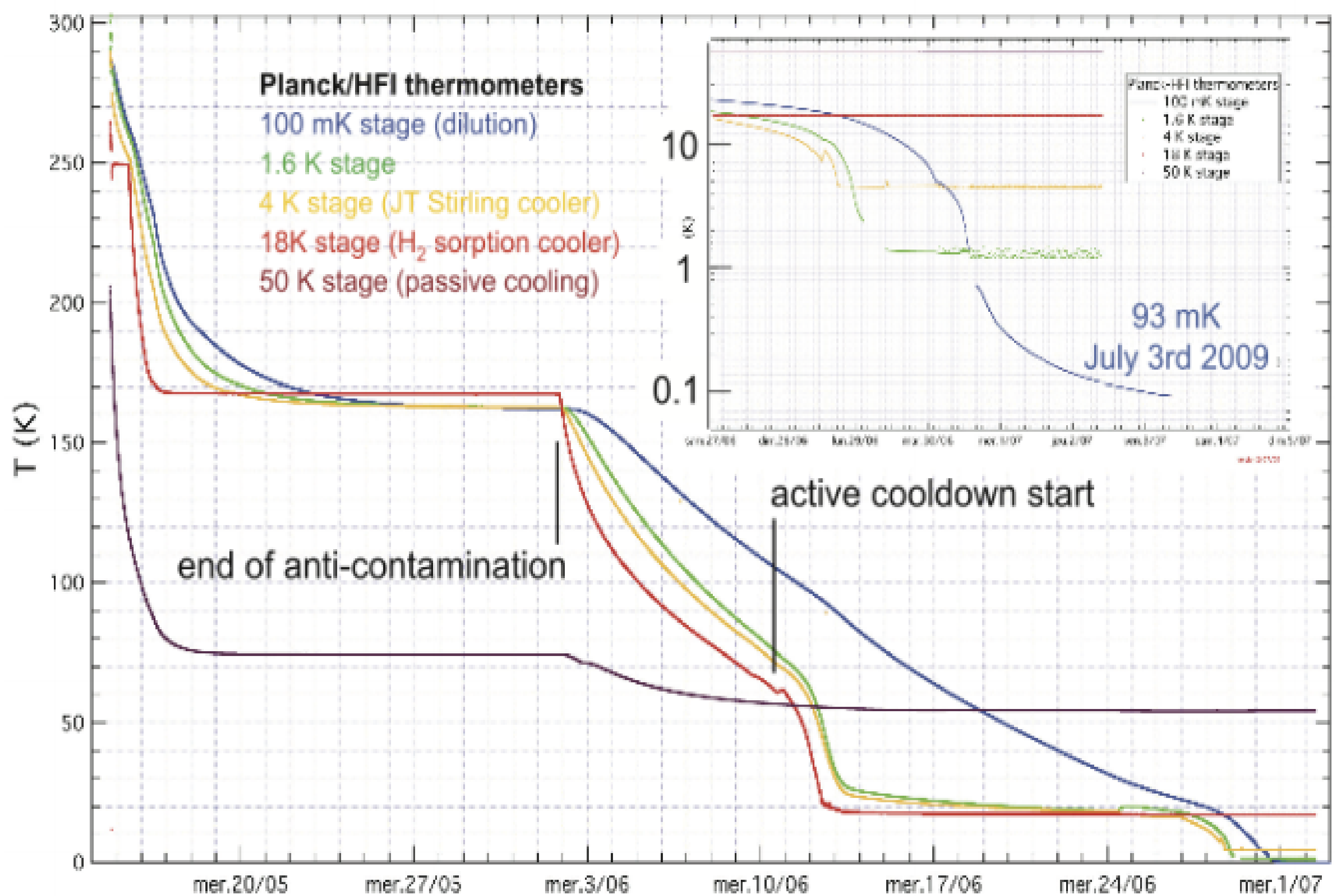

Planck HFI data flow chart

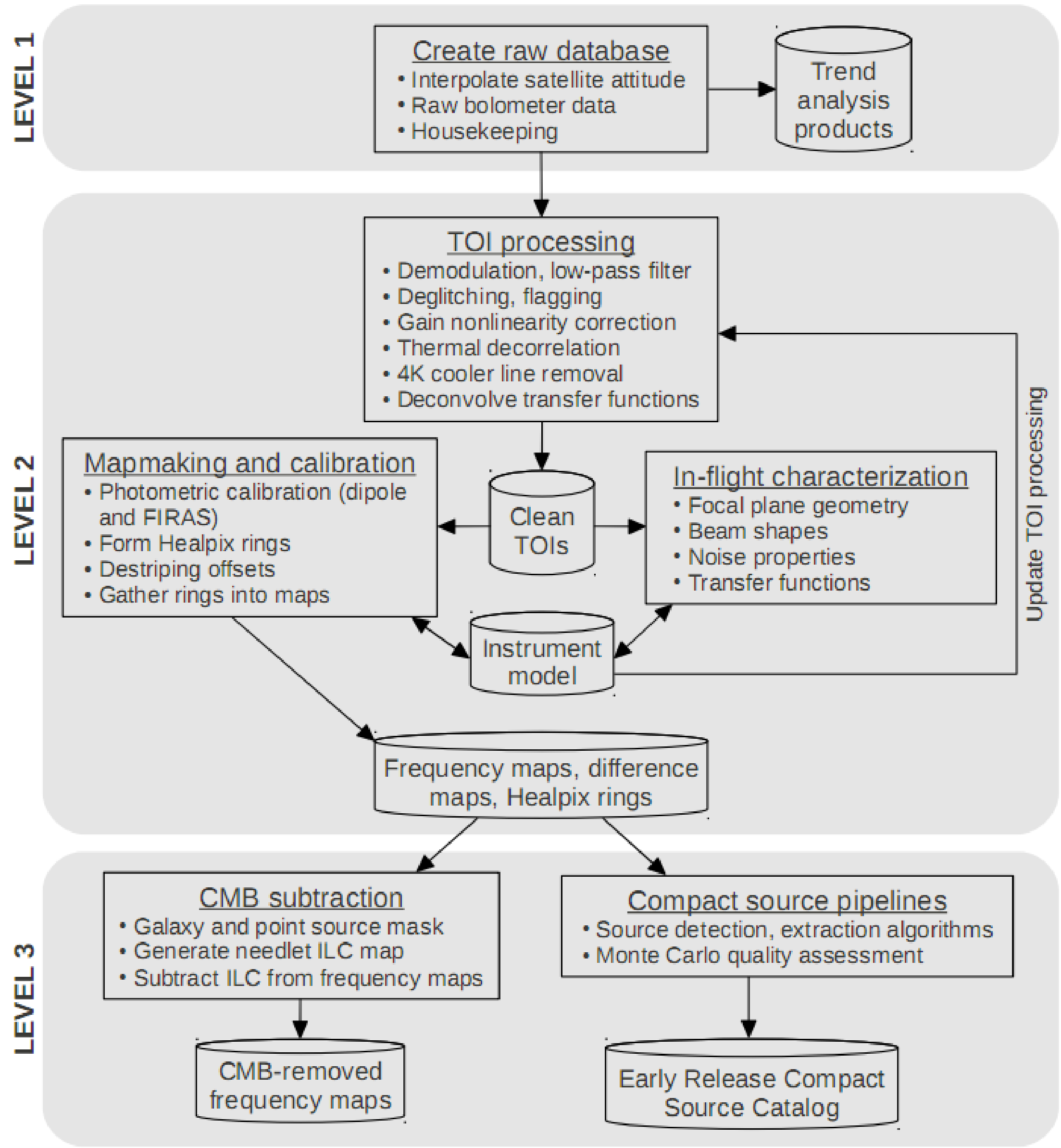

Cosmic ray interaction

HFI Core Team: HFI Data Processing

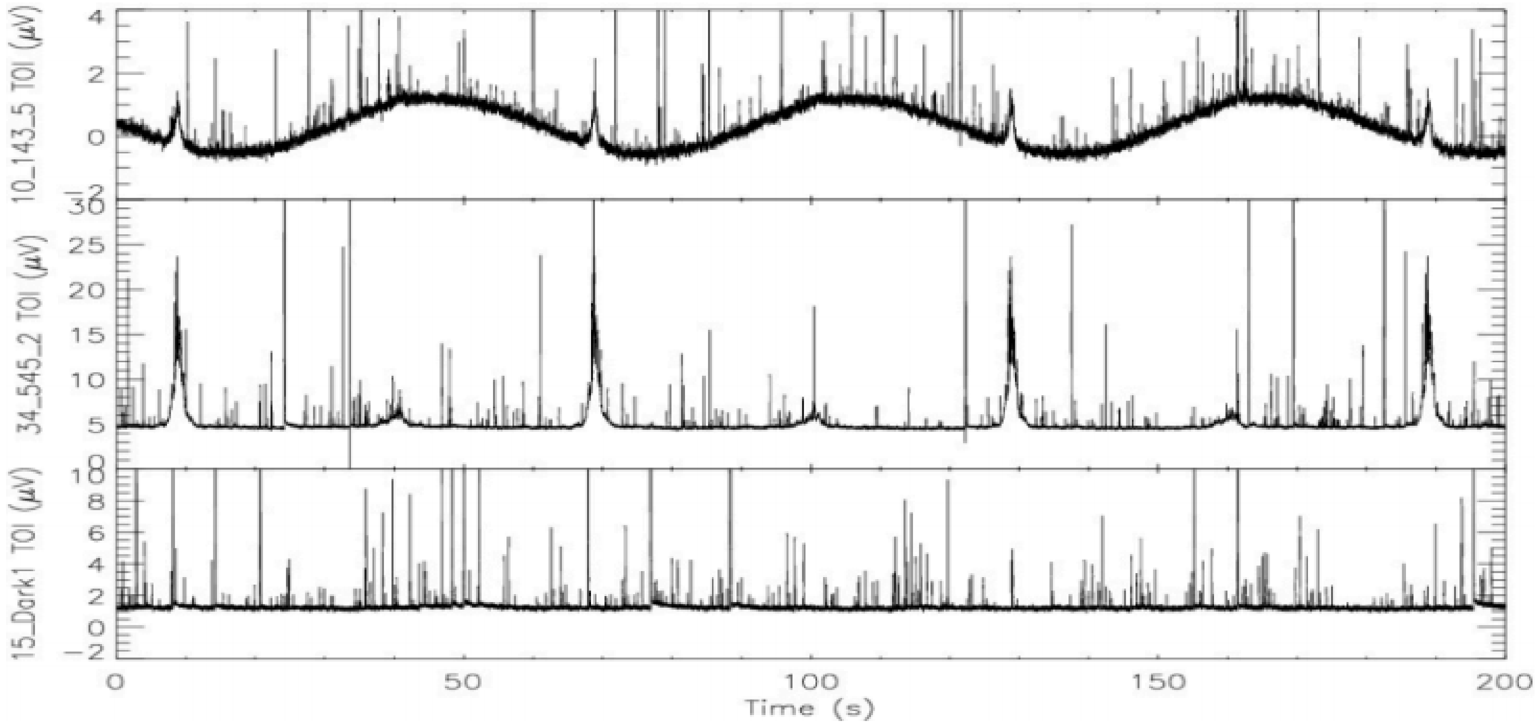

Figure 4. Raw TOIs for three bolometers, the '143-5' (top), '545-2' (middle), and 'Dark1' (bottom) illustrating the typical behaviour of a detector at 143 GHz, 545 GHz, and a blind detector over the course of three rotations of the spacecraft at 1 rpm. At 143 GHz, one clearly sees the CMB dipole with a 60 s period. The 143 and 545 GHz bolometers show vividly the two Galactic Plane crossings, also with 60 s periodicity. The dark bolometer exhibits a nearly constant baseline together with a population of glitches from cosmic rays similar to those seen in the two upper panels.

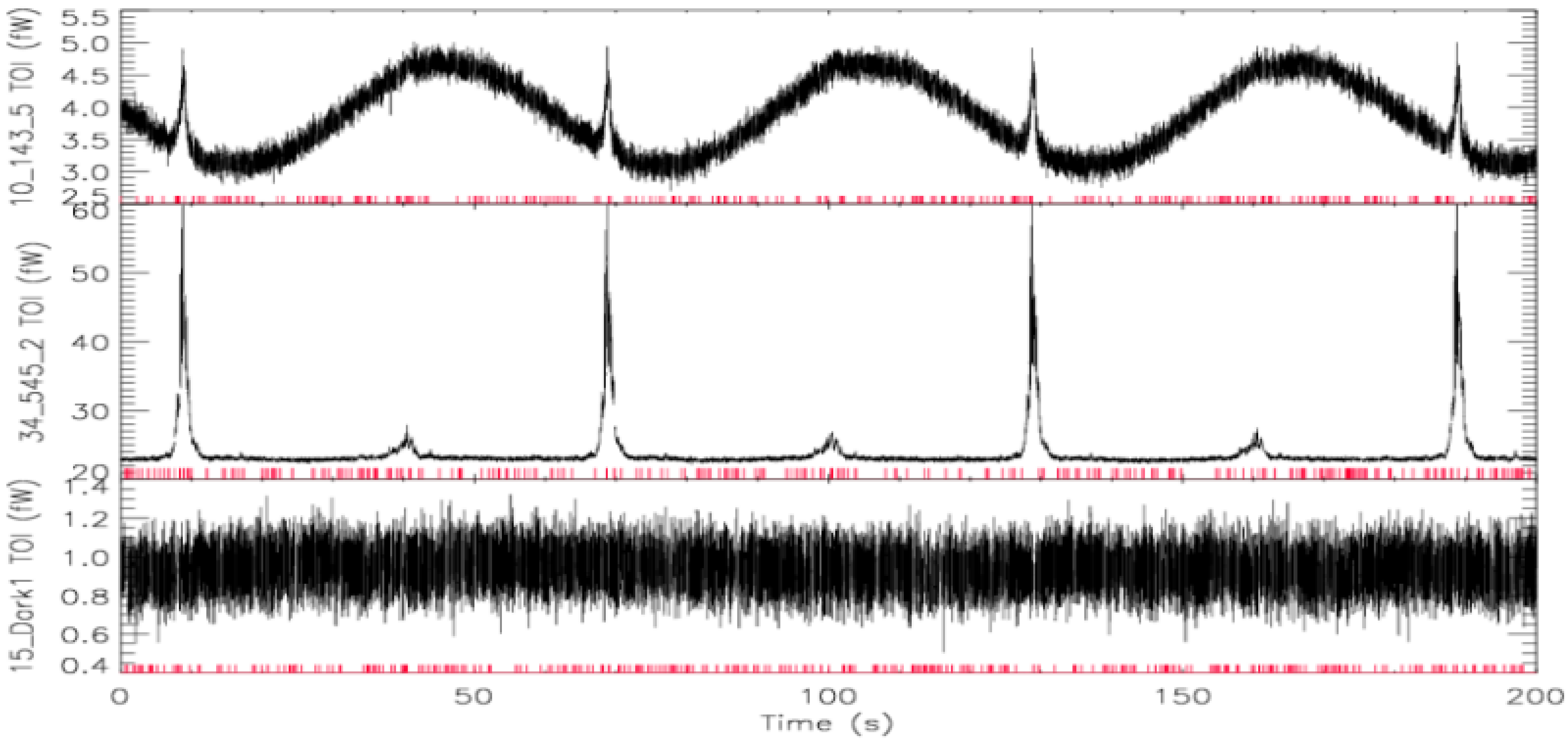

Figure 19. Processed TOI for the same bolometers and time range as shown in Fig. 4. Red samples are considered valid. Times where data are flagged, are indicated by the purple ticks at the bottom of each plot.

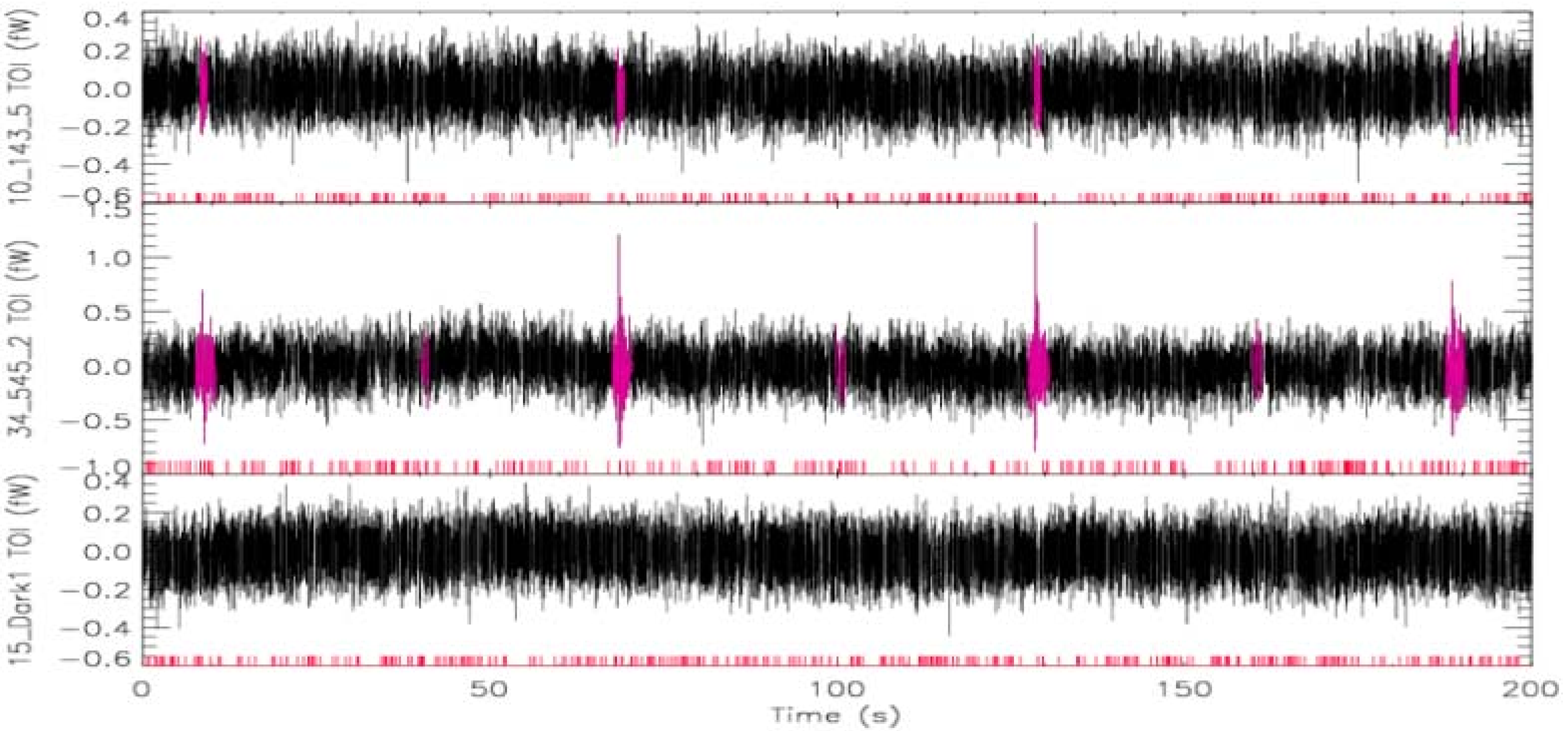

Figure 20. Processed TOI as in Fig. 19, but with the ring averaged signal subtracted to enhance features near the noise limit. Times where data are flagged, are shown by the purple lines at the bottom of each plot. Purple zones show where the strong signal Flag is set, where the phase-bin ring average subtraction is not expected to yield a perfect signal cancellation.

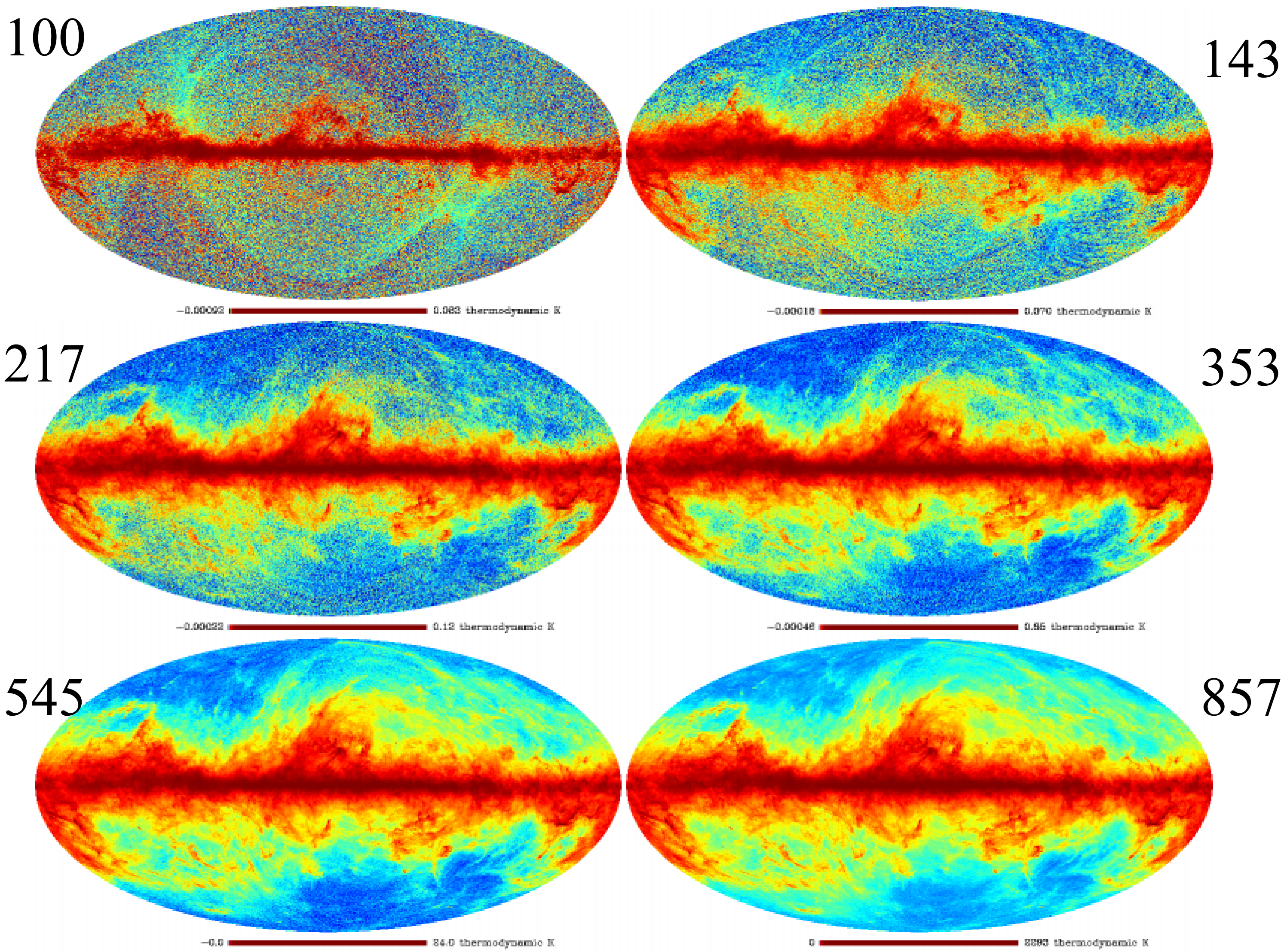

Figure 43. CMB-removed channel maps. From left to right and then top to bottom, the maps correspond to the 100, 143, 217, 350, 545, and 857 GHz.

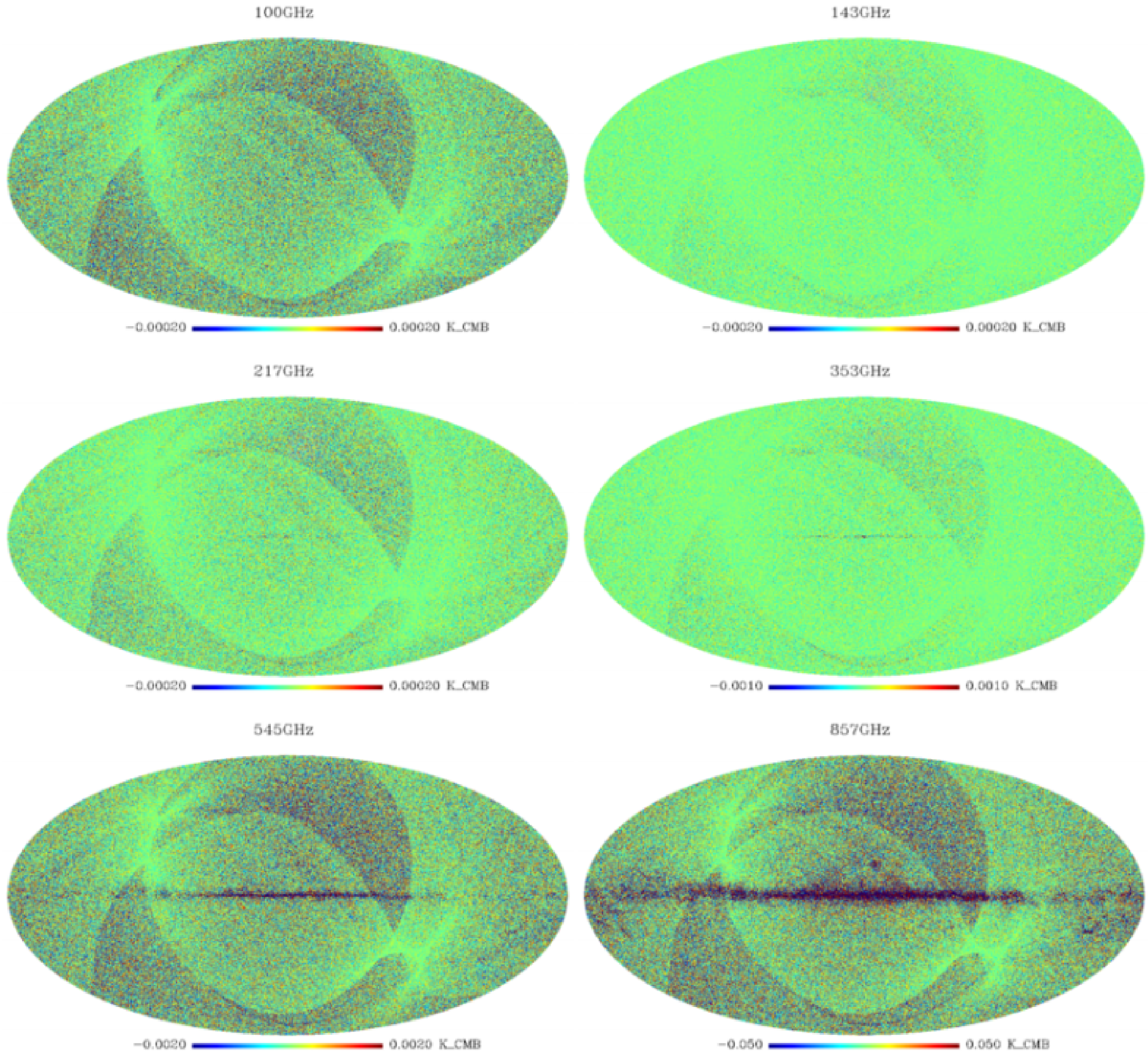

Figure 34. Residual maps of the half differences between the maps made from the first and second half rings projection (*from top left to bottom right:* 100, 143, 217, 353, 545, 857 GHz) in 1.7 arcmin pixels (Nside= 2048). Note that the CMB channels at 100-217 GHz are all shown on the same color scale. In addition the noise pattern, which is well traced by the hit maps of fig. 33, one also see the small differences (relative to the signal), when gradients of the signal are large (mostly in the Galactic plane) and sub-pixel effects become quite apparent.

Planck HFI in-flight sensitivity

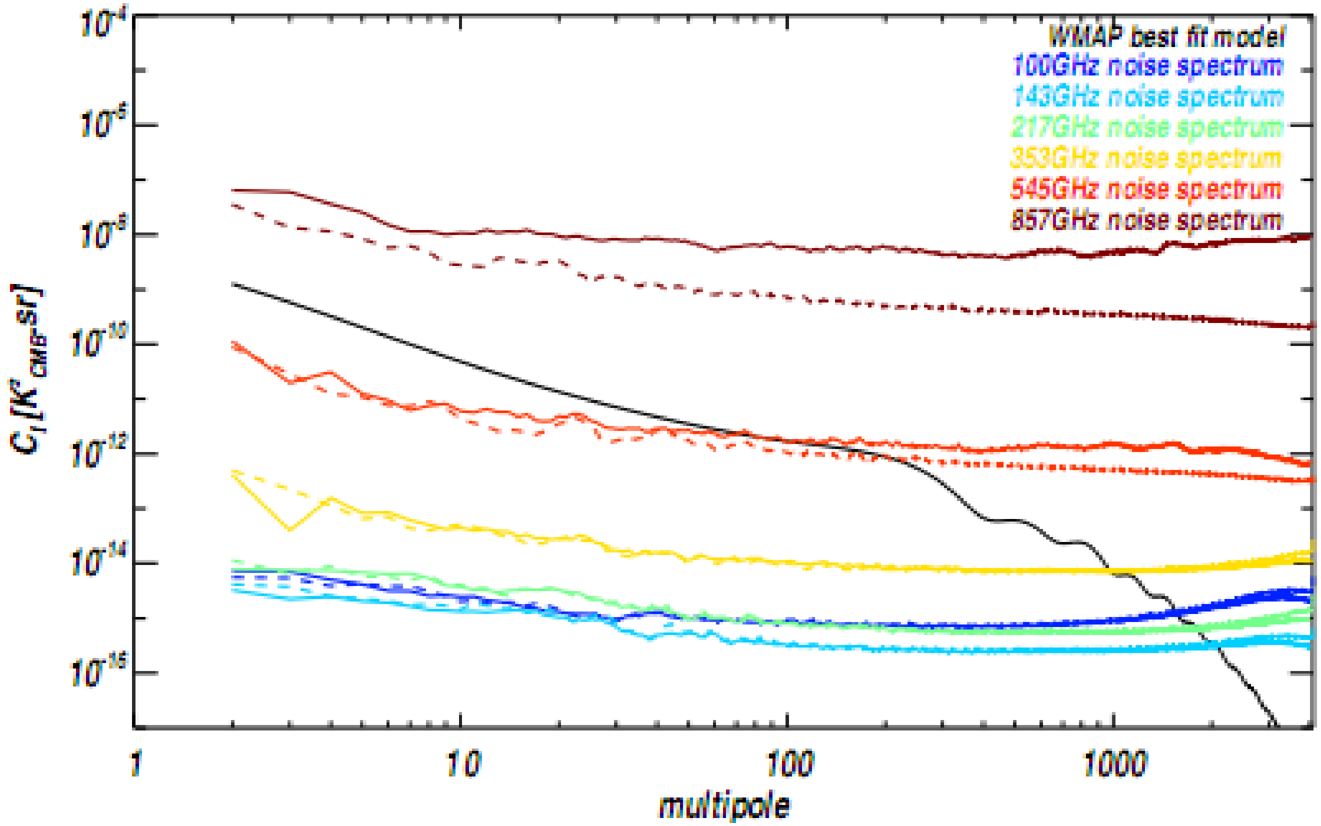

Figure 35. Power spectra from the difference maps shown on Fig. 34, on the full sky (*solid line*) and after masking the Galactic plane (*dashed line*). The sky coverage correction was done according to Tristram et al. (2005). As expected, the difference is only substantial at high frequency, when gradients of the Galactic signal are large.

Comparison with Blue Book

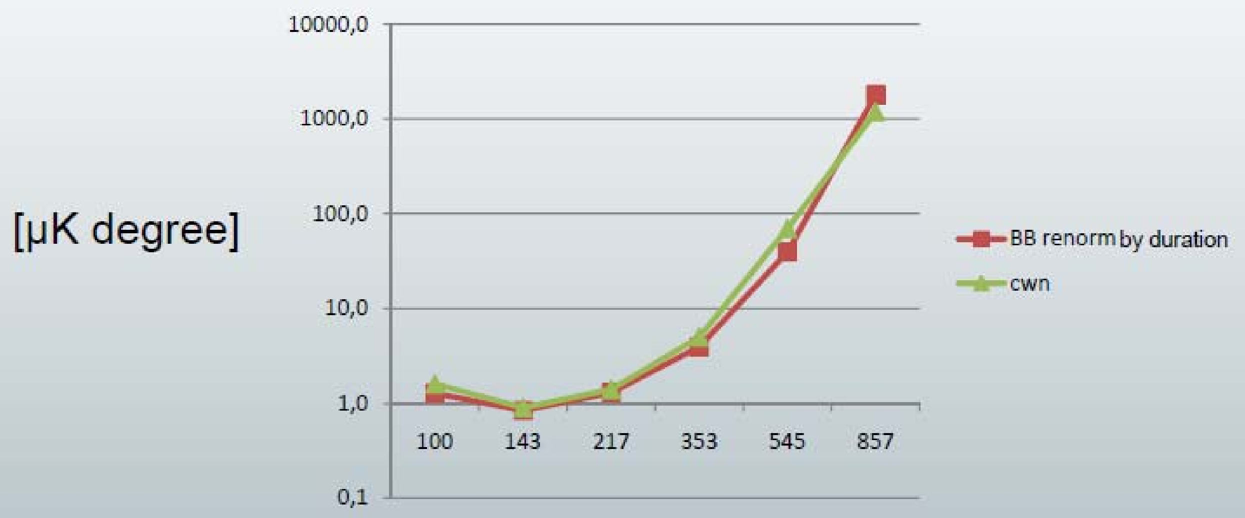

The combination of residual excess low frequency noise and better than the goals NETs leads to current maps whose high frequency noise is rather close to goal values ☺

Comparison Blue Book / WMAP

PLANCK	LFI			HFI					
Center Freq (GHz)	30	44	70	100	143	217	353	545	857
Angular resolution (FWHM arcmin)	33	24	14	10	7.1	5.0	5.0	5	5
Sensitivity in I [μK.deg] [$\sigma_{pix}\ \Omega_{pix}^{1/2}$]	3.0	3.0	3.0	1.1	0,7	1.1	3.3	33	3.0

WMAP Center Freq.	23	33	41	61	94
Angular resolution (FWHM arcmin)	49	37	29	20	12,6
Sensitivity in I [μK.deg], 1 yr (8 yr)	12.6 (4.5)	12.9 (4.6)	13.3 (4.7)	15.6 (5.5)	15.0 (5.3)

The aggregated sensitivity of Planck core CMB channels is ~0.5μK.deg in T (nominal mission - 14months)

NB: Anticipated survey duration is now ~30 months, so final sensitivity ~0.33 μK.deg in T (approx 1000 years of WMAP 60+90GHz aggregated sensitivity of 10.8 μK.deg in1yr)

Planck first light

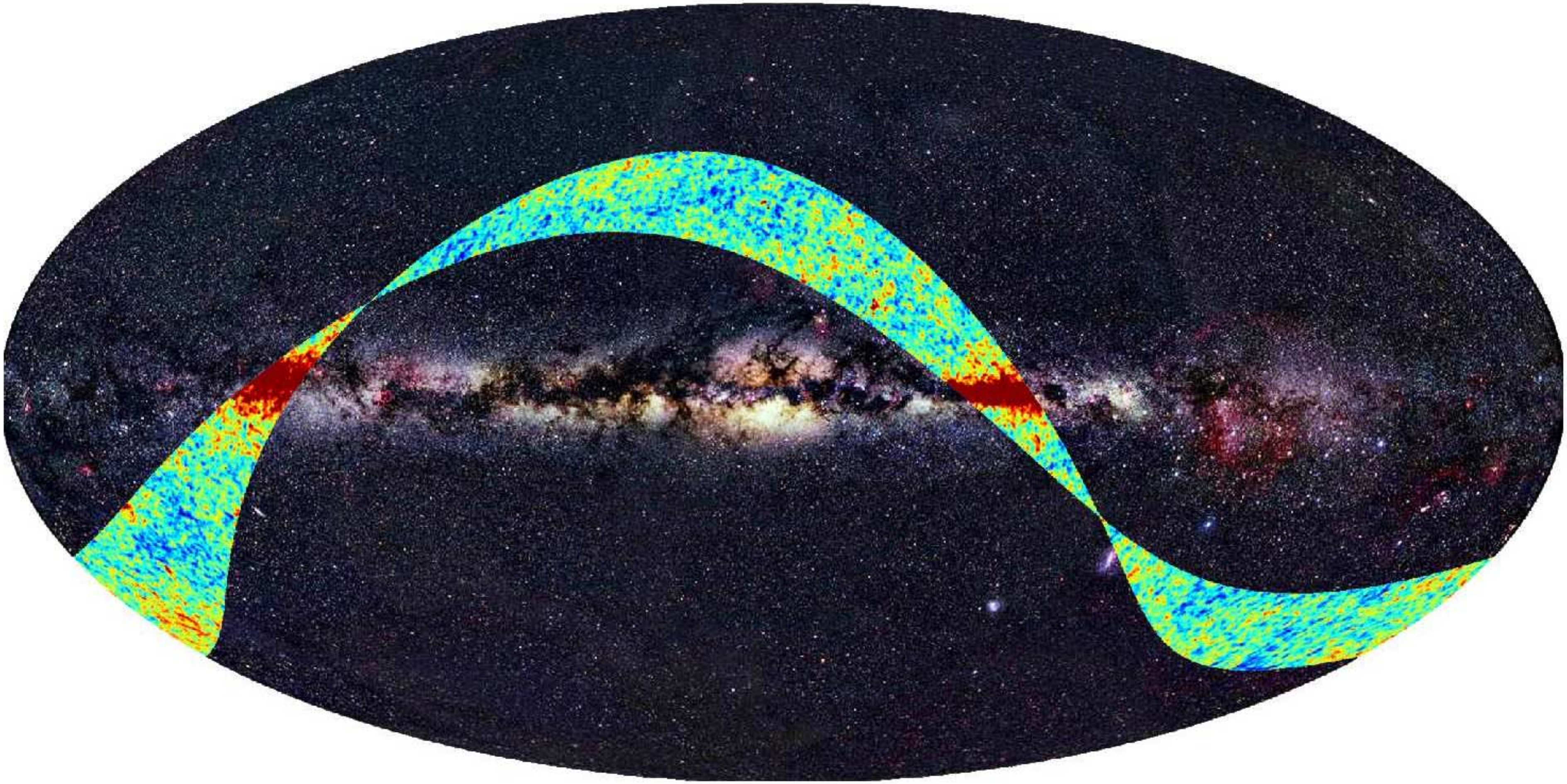

Comparison with a sky photo in the visible

ESA, Planck HFI & LFI consortia, and Axel Mellinger

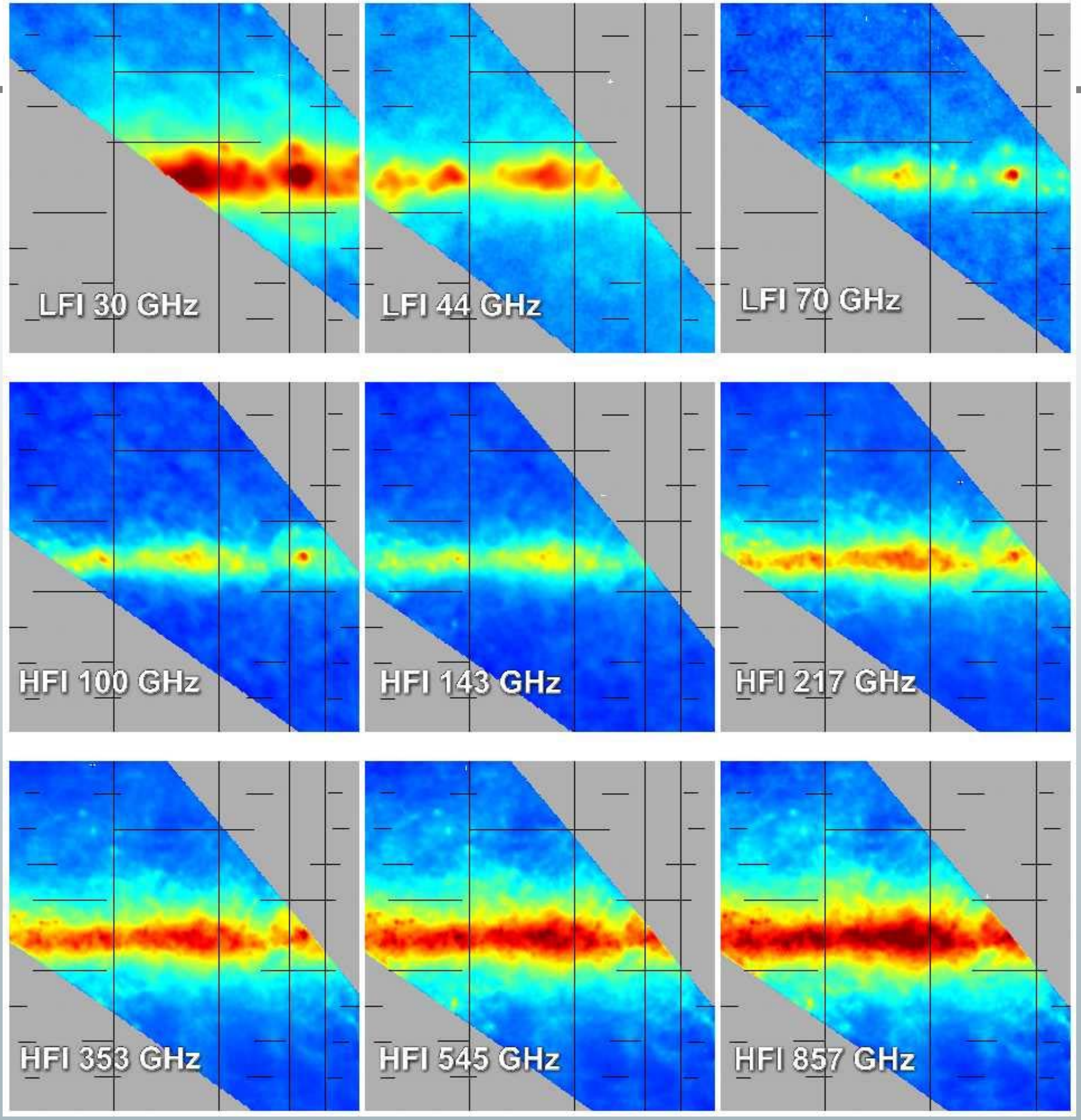
LFI 30 GHz
LFI 44 GHz
LFI 70 GHz
HFI 100 GHz
HFI 143 GHz
HFI 217 GHz
HFI 353 GHz
HFI 545 GHz
HFI 857 GHz

Outside the galactic plane

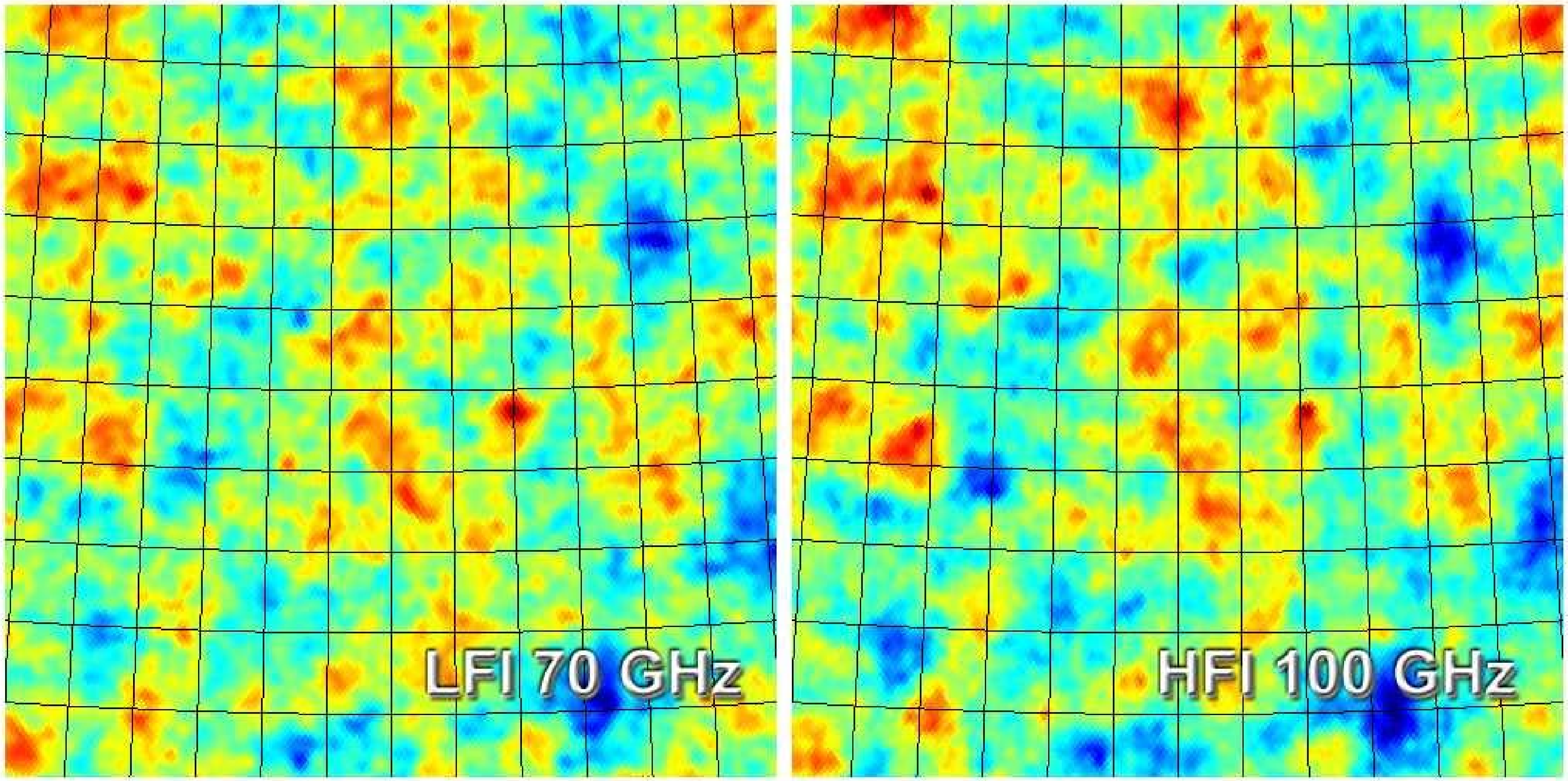

10x10 degrees^2

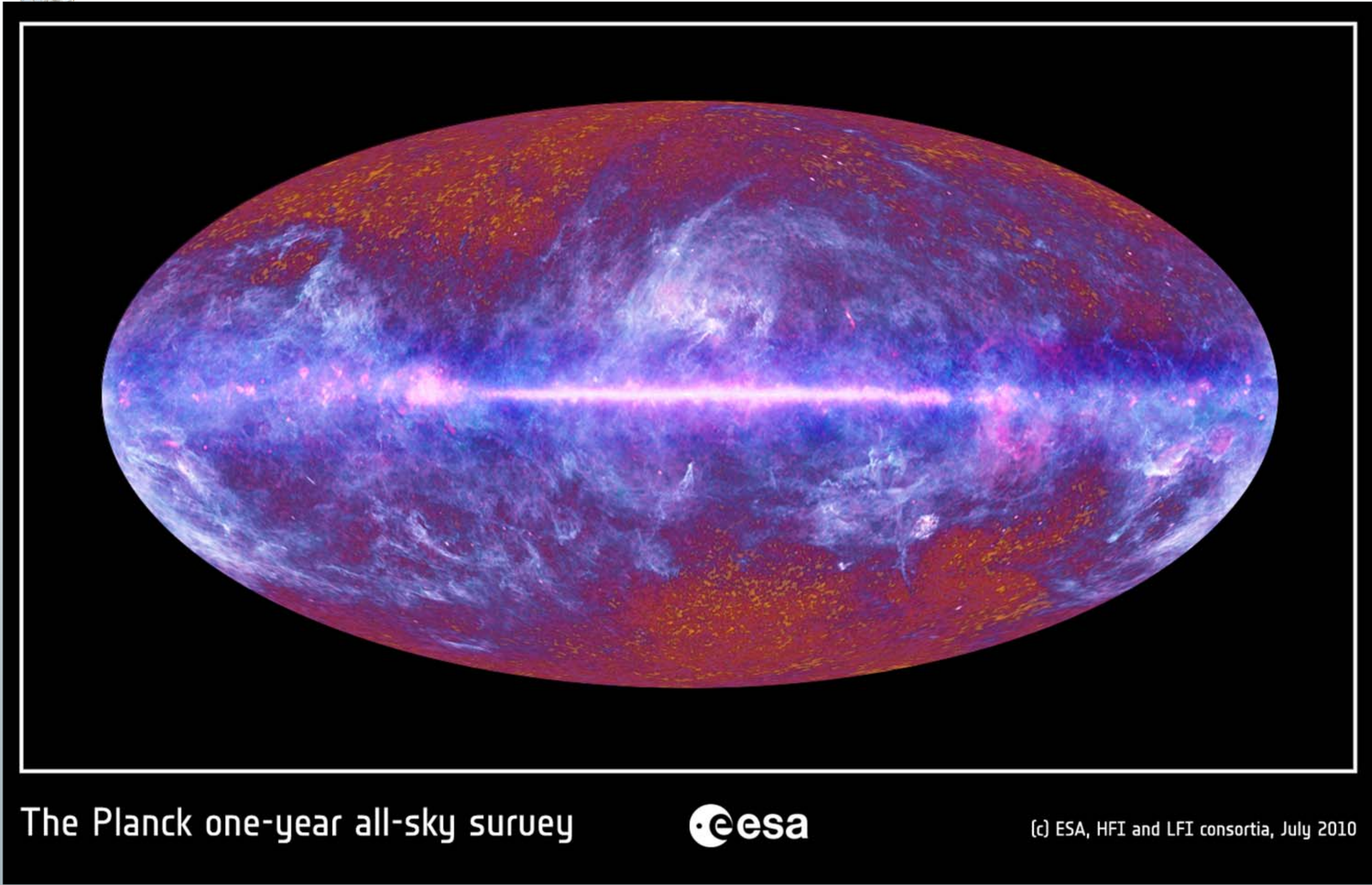
The Planck one-year all-sky survey
esa
(c) ESA, HFI and LFI consortia, July 2010

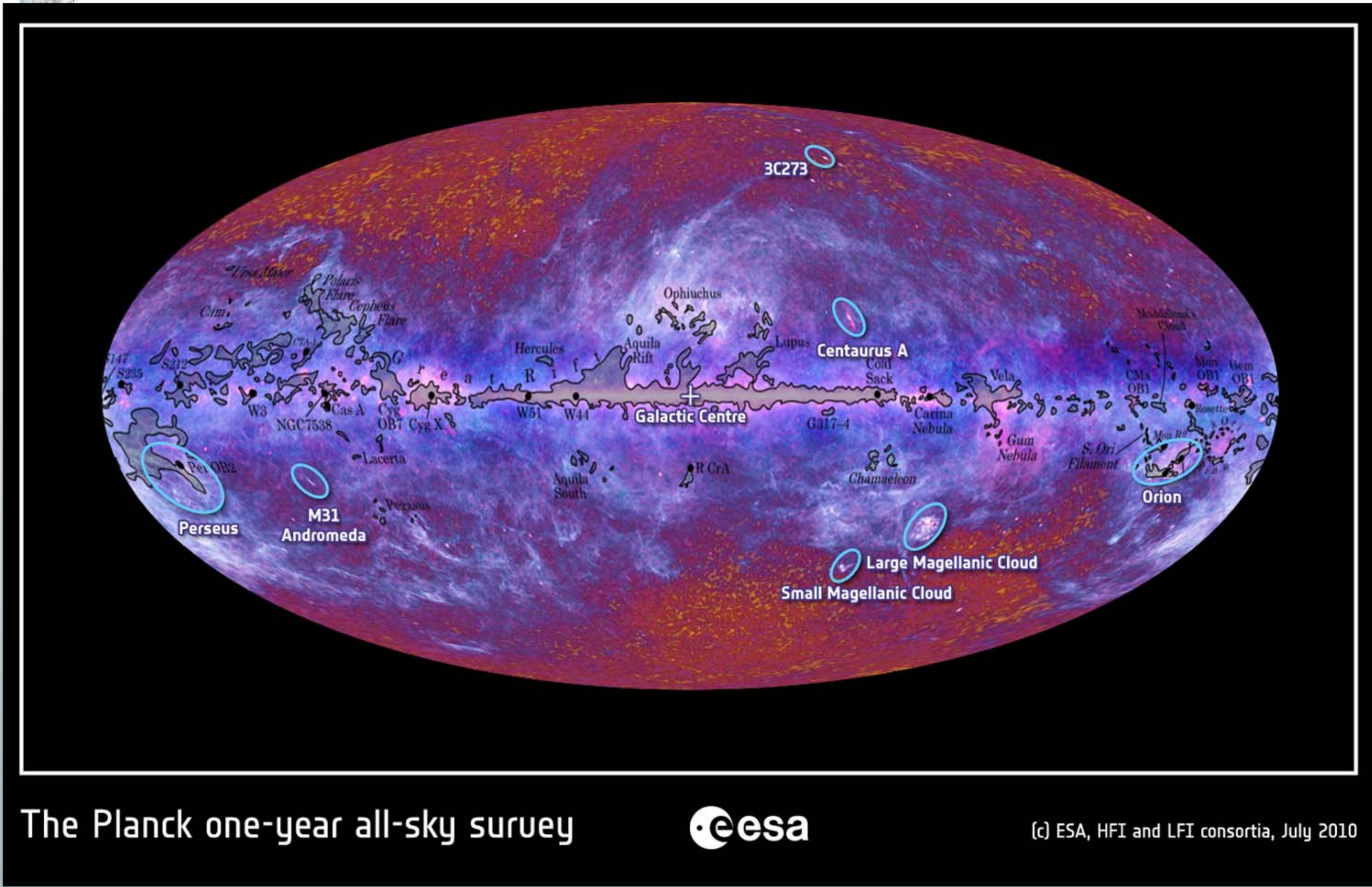
3C273
Ophiuchus
Polaris Flare
Cepheus Flare
Ursa Major
Lupus
Centaurus A
Hercules
Aquila Rift
Great Rift
Coal Sack
Vela
CMa OB1
Mon OB1
Gem OB1
Rosette
S147
S235
S212
W3
NGC7538
Cas A
Cyg OB7
Cyg X
W51
W44
Galactic Centre
G317-4
Carina Nebula
Gum Nebula
S. Ori Filament
Per OB2
Lacerta
Pegasus
Aquila South
R CrA
Chamaeleon
Orion
Perseus
M31
Andromeda
Large Magellanic Cloud
Small Magellanic Cloud
The Planck one-year all-sky survey
esa
(c) ESA, HFI and LFI consortia, July 2010

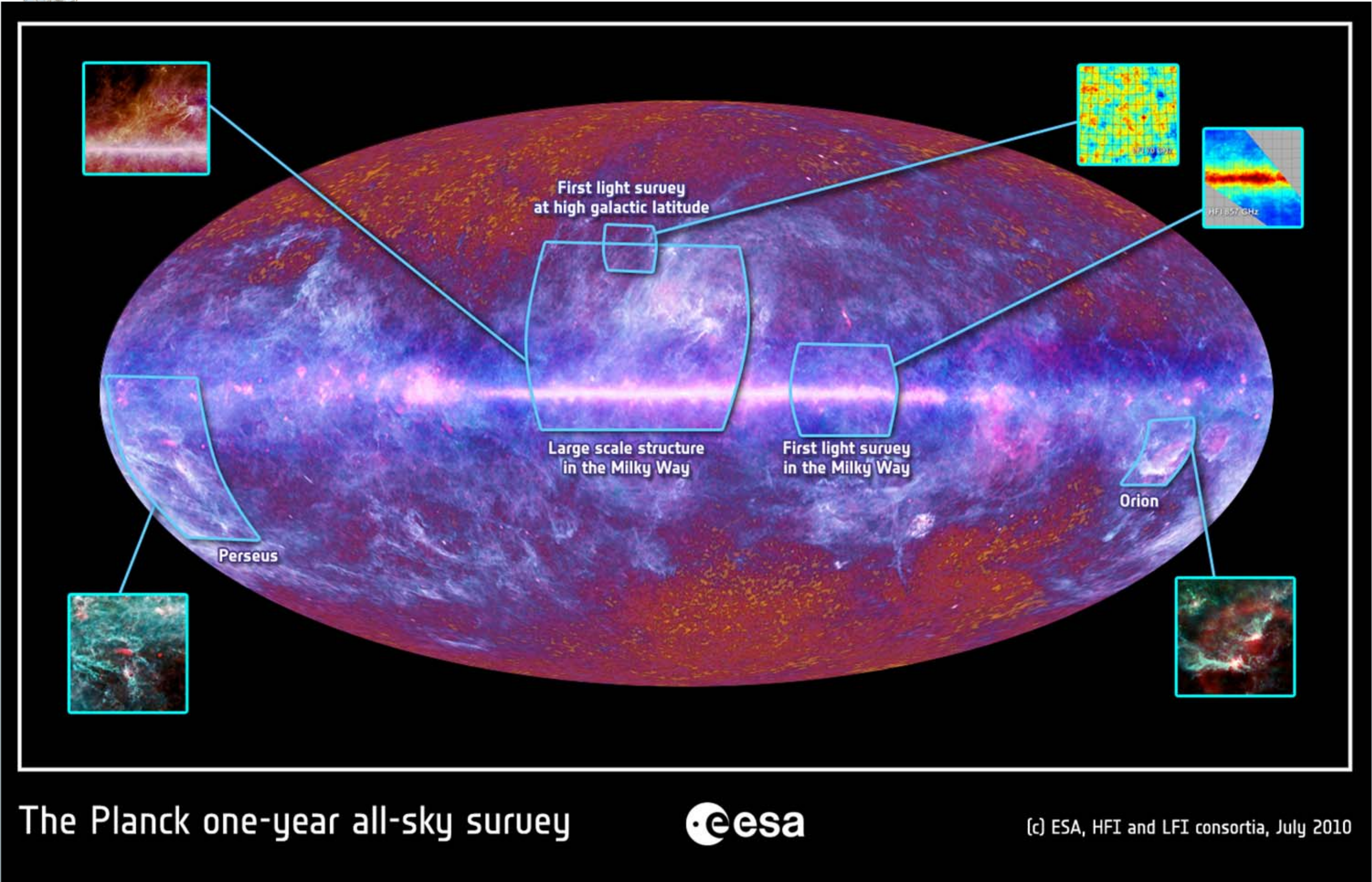
First light survey
at high galactic latitude
Large scale structure
in the Milky Way
First light survey
in the Milky Way
Perseus
Orion
HFI 857 GHz
The Planck one-year all-sky survey
esa
(c) ESA, HFI and LFI consortia, July 2010

Spectrum of Interstellar Dust

IRAS DIRBE HFI WMAP LFI

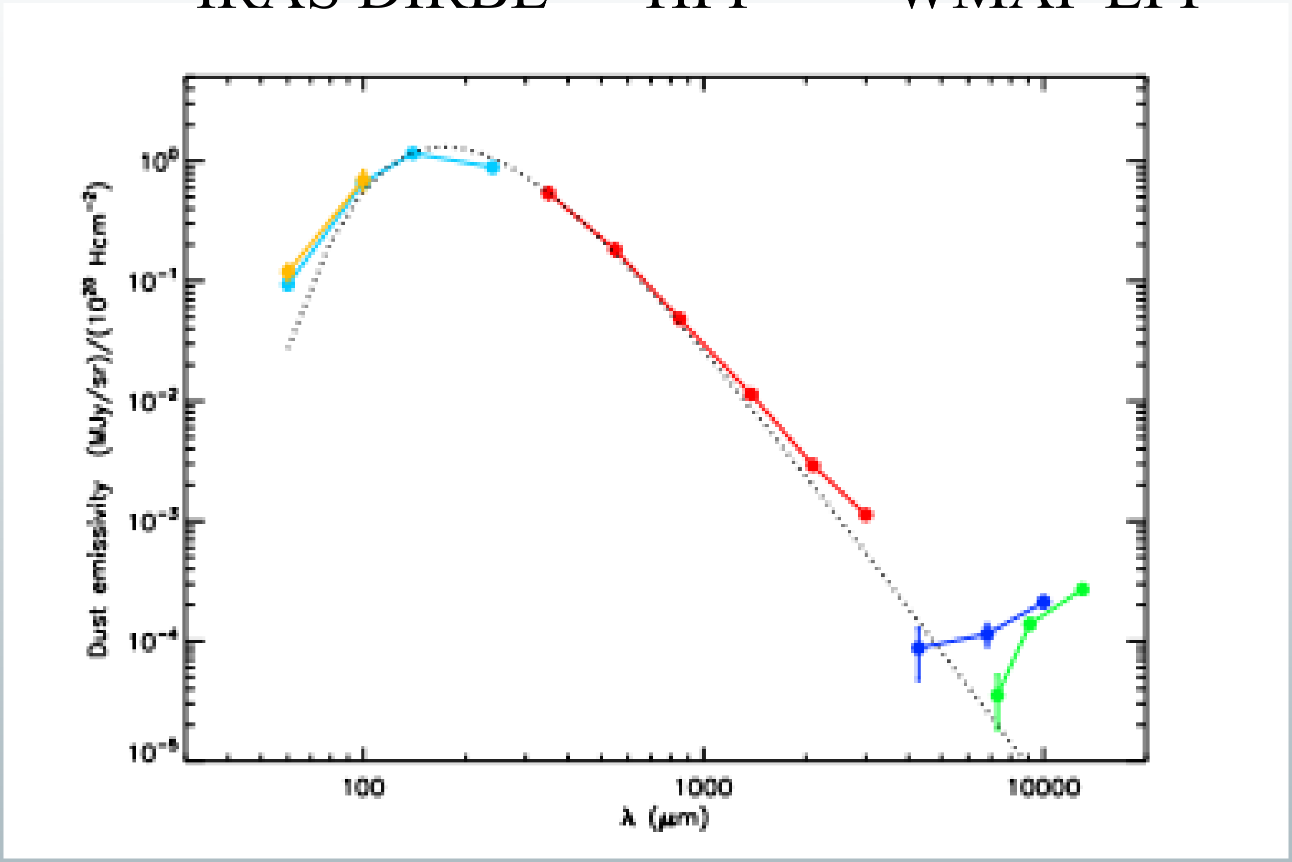

Dust temperature

T_D changes
because emissivity changes
not because
the radiation field changes

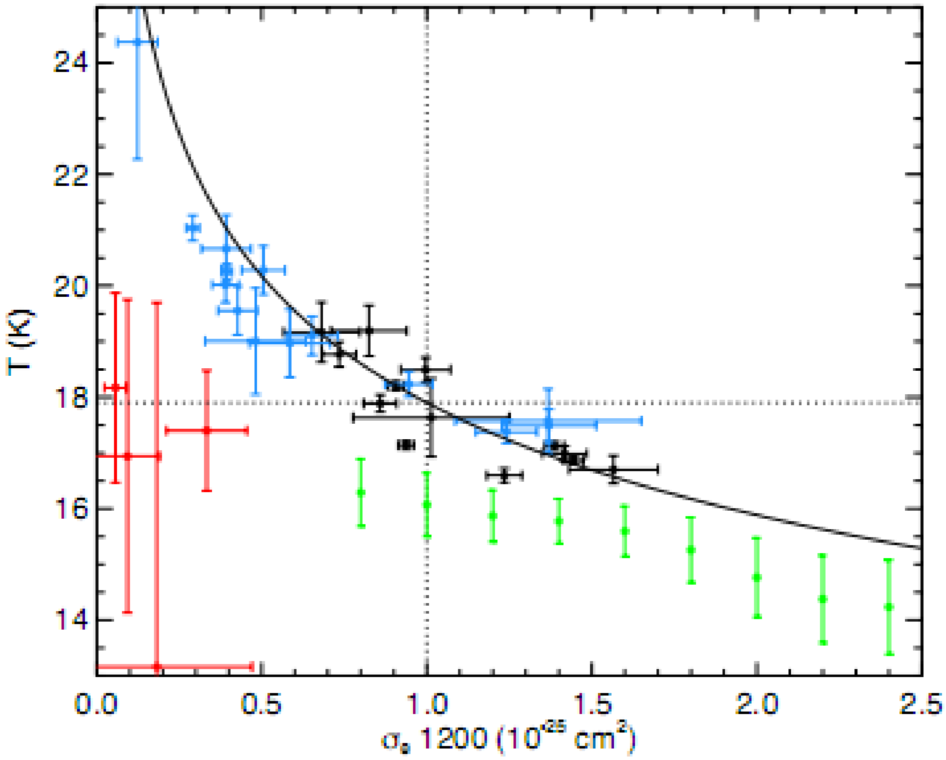

Fig. 16. Temperature vs emission cross section estimated from 545 to 3000 GHz with $\beta = 1.8$. Black is local, blue is IVCs, red is HVCs and green is the data points obtained on the Taurus molecular clouds (Planck Collaboration 2011u). For the latter the error bars give the dispersion of T in each bin of σ_e. The solid line respresent a constant emitted energy for the diffuse ISM reference values ($\sigma_e = 1 \times 10^{-25}$ cm^{-2} and $T = 17.9$ K - dotted lines).

Filaments by Herschel

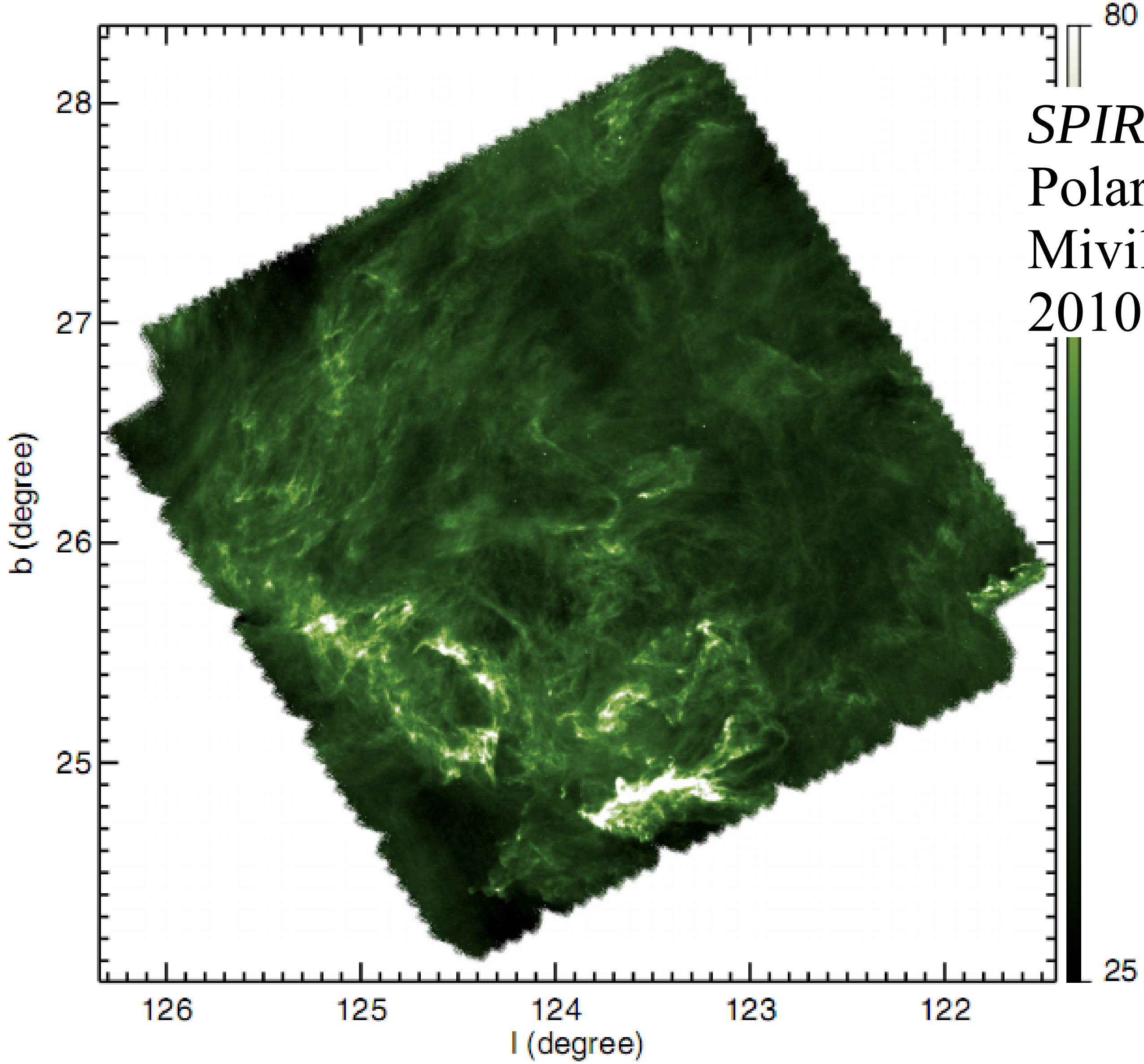

SPIRE 250micron
Polaris Flare
Miville-Deschênes et al
2010, AA, 518, L104

Global Emission of the Milky Way

857 GHz

The *Planck* collaboration: Properties of the interstellar medium in the Galactic plane

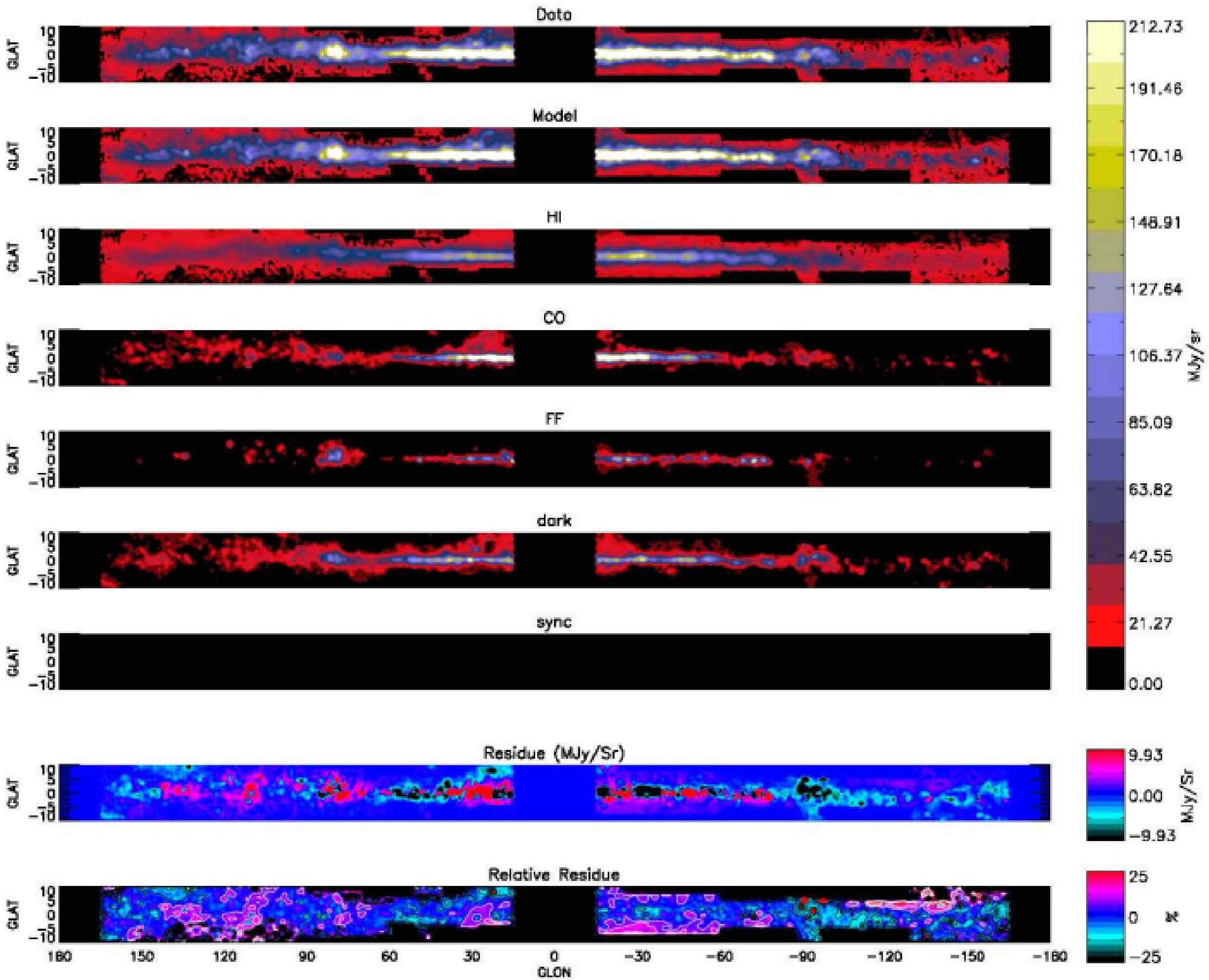

Fig. 3. Results of the inversion for the 857 GHz band. From top to bottom are the: observed emission, modelled emission, atomic contribution, molecular contribution, ionised contribution, dark gas contribution, synchrotron contribution, residual, and relative residual. All images except for the residual maps are at the same intensity scale. Contours are drawn on the relative residual map every 5%. The centre and anti-centre regions have been masked as the kinematic distance method is inapplicable to these regions.

30 GHz

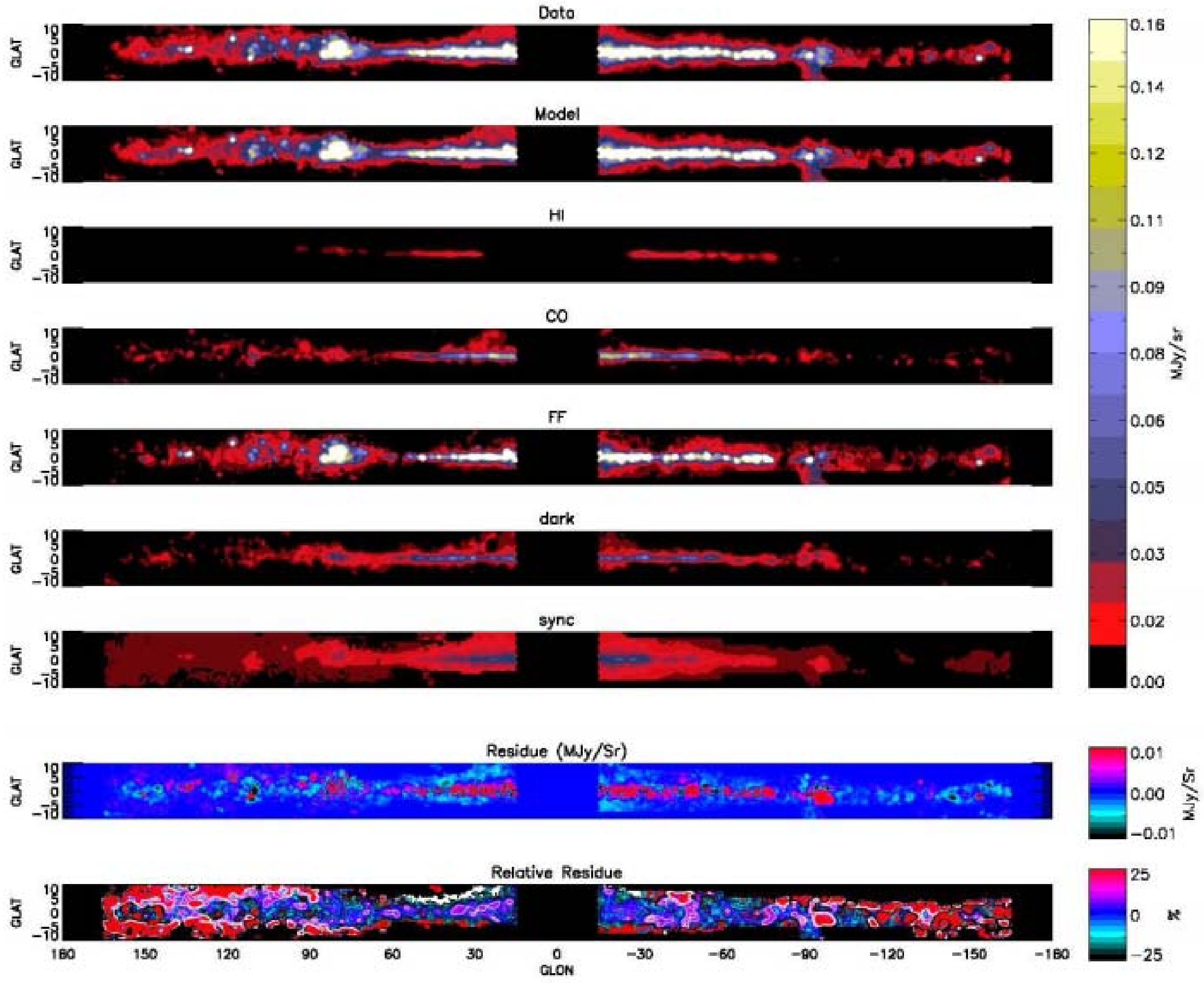

Fig. 4. Same as Fig. 3 for the 30 GHz band.

Spinning Dust?

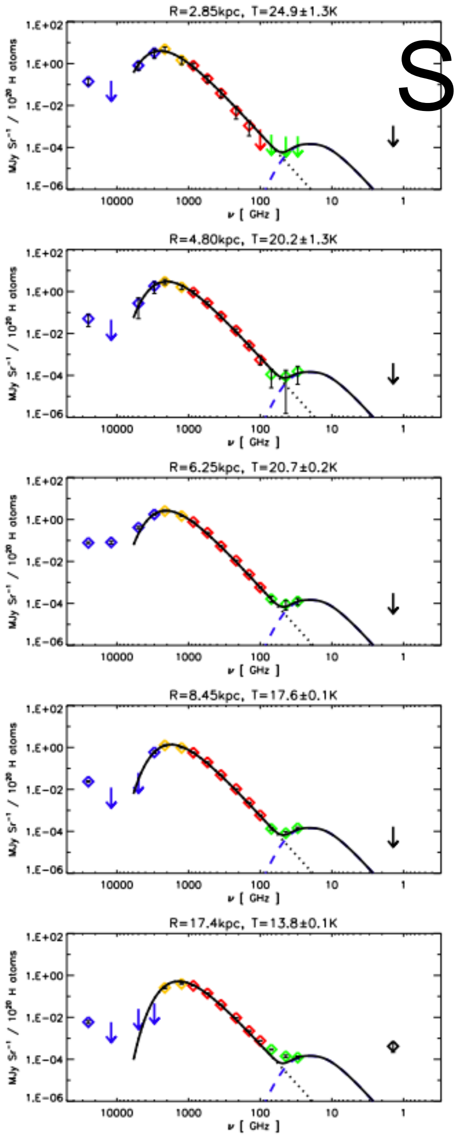

Fig. 6. SEDs for the atomic component, each sorted in increasing Galactocentric radius. The colour of the symbols refer to the mission the data came from: *IRAS* (blue), *DIRBE* (yellow), HFI(red), LFI(green) and 1.4 GHz (black). The SEDs also show various fitted laws: the dotted line is the thermal dust SED, the short dashed line spinning dust in an atomic medium, and the solid line the sum of all contributions. The spinning dust contribution is not a fit, but simply the result of using typical values in the model (see Sect. 4.2.3 for details). The point at 1.4 GHz in the outer Galaxy is most likely false, and due to crosstalk between the atomic and synchrotron template.

Atomic

Molecular

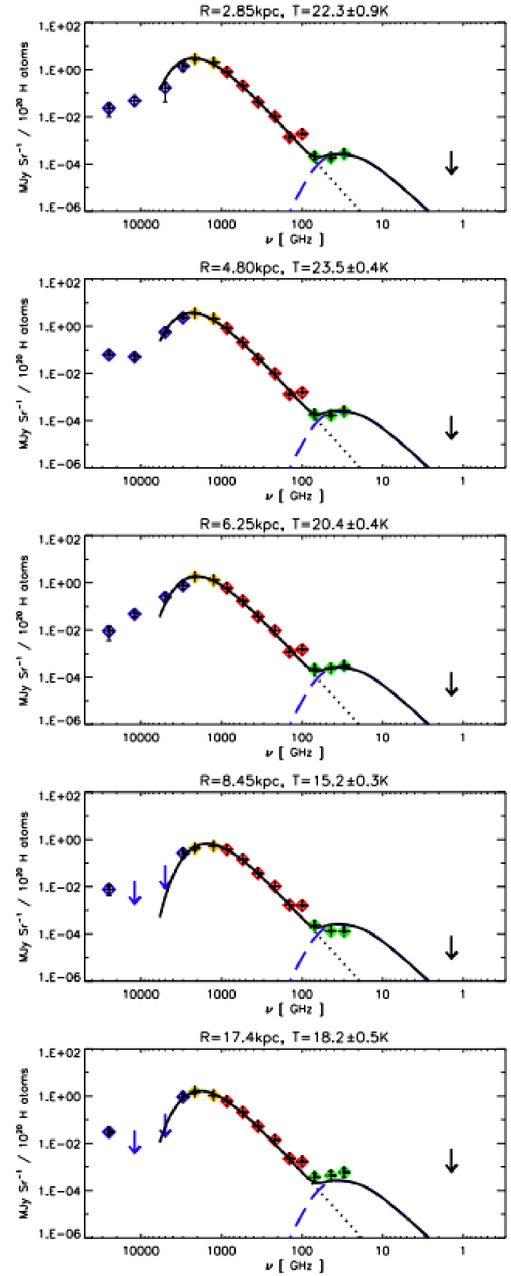

Fig. 7. SEDs for the CO component, each sorted in increasing Galactocentric radius. The different lines and colours are as described in Fig. 6 except for the long dashed line which represents spinning dust in a molecular medium.

First public Planck data

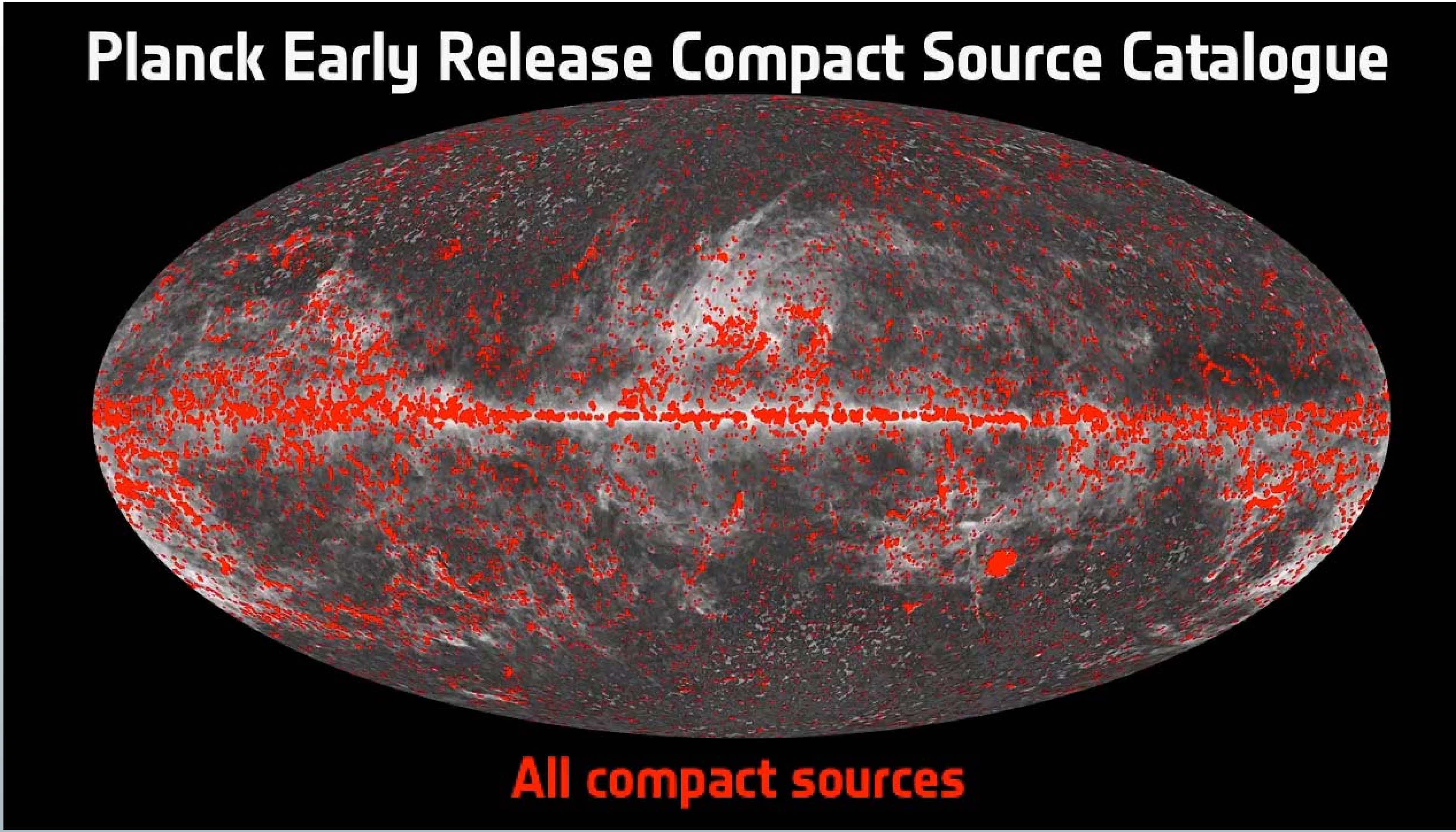

15000 sources. >200-600 mJy (10 sigma), +ECC, ESZ

Sunyaev-Zel'dovich effect

Compton parameter: y ~ N T

Y=integral (y dOmega) ~ Mg T ~ $M^{5/3}$

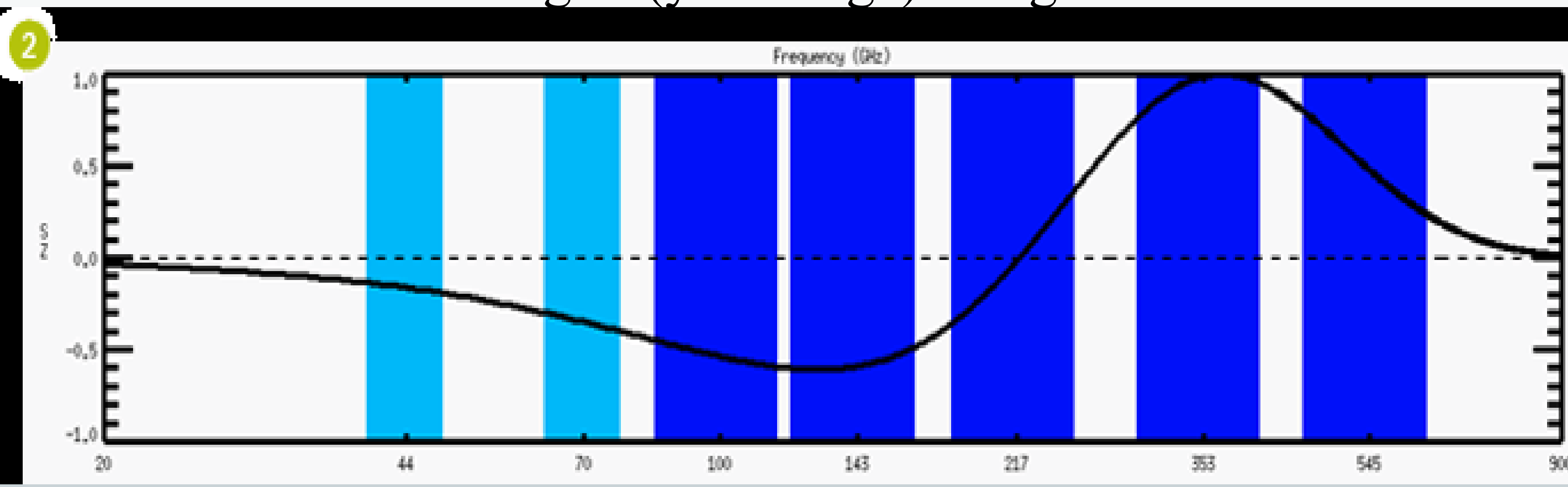

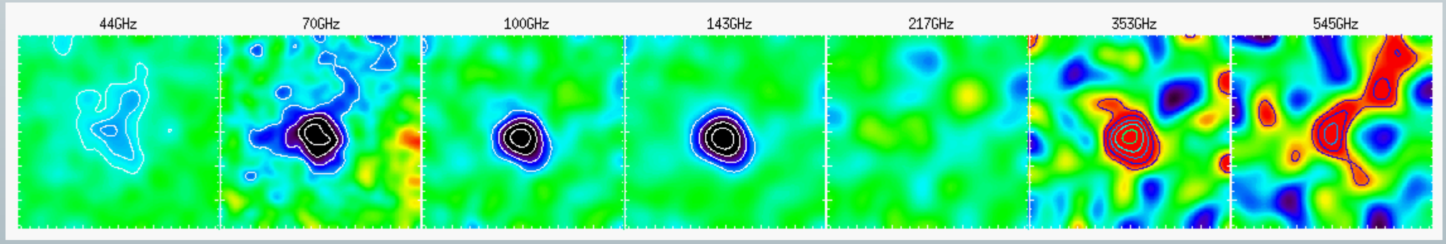

A2319

Coma Cluster of galaxies

Coma

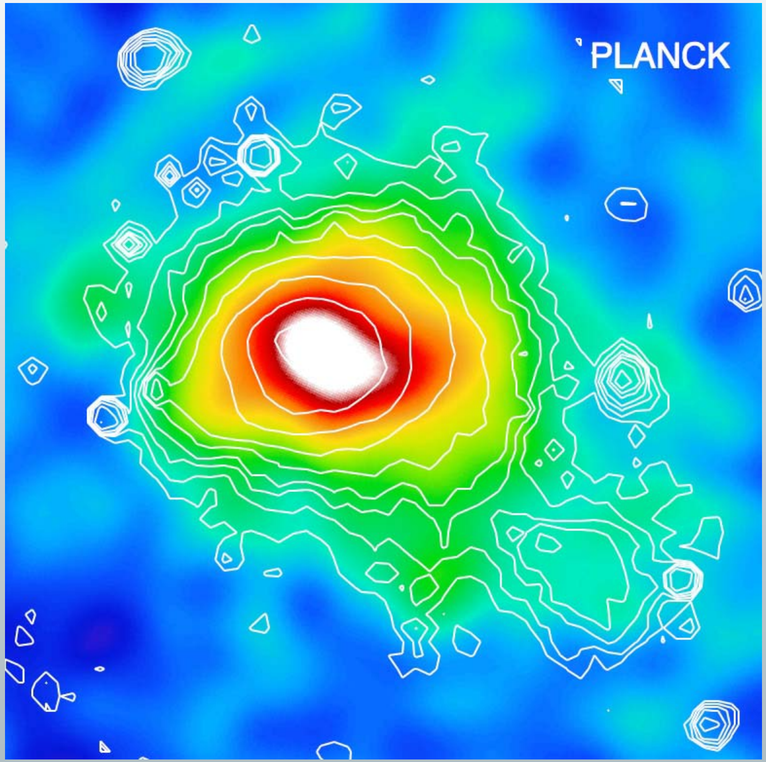

HST - Visible

Planck (color) & XMM (contours)

199 clusters detected by Planck

Planck Collaboration: The *Planck* all-sky Early Sunyaev-Zeldovich cluster sample

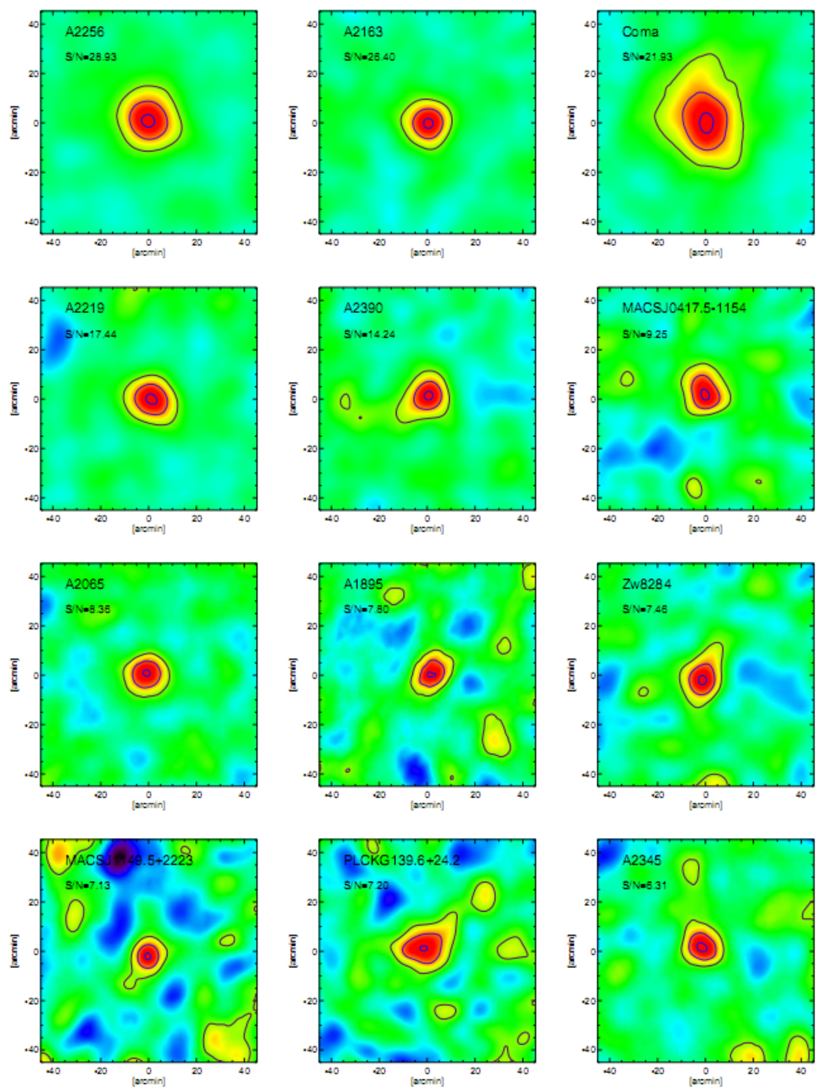

Fig. 6. Illustrations of reconstructed *y*-maps (1.5° × 1.5°, smoothed to 13 arcmin) for clusters spanning S/N from 29 to 6 from the upper left to the lower right.

199 robust detections
30 new clusters
Most are Rosat clusters
first SZ detection
z<0.7

Follow-up by XMM-Newton

Planck Collaboration: *XMM-Newton* follow-up for validation of *Planck* cluster candidates

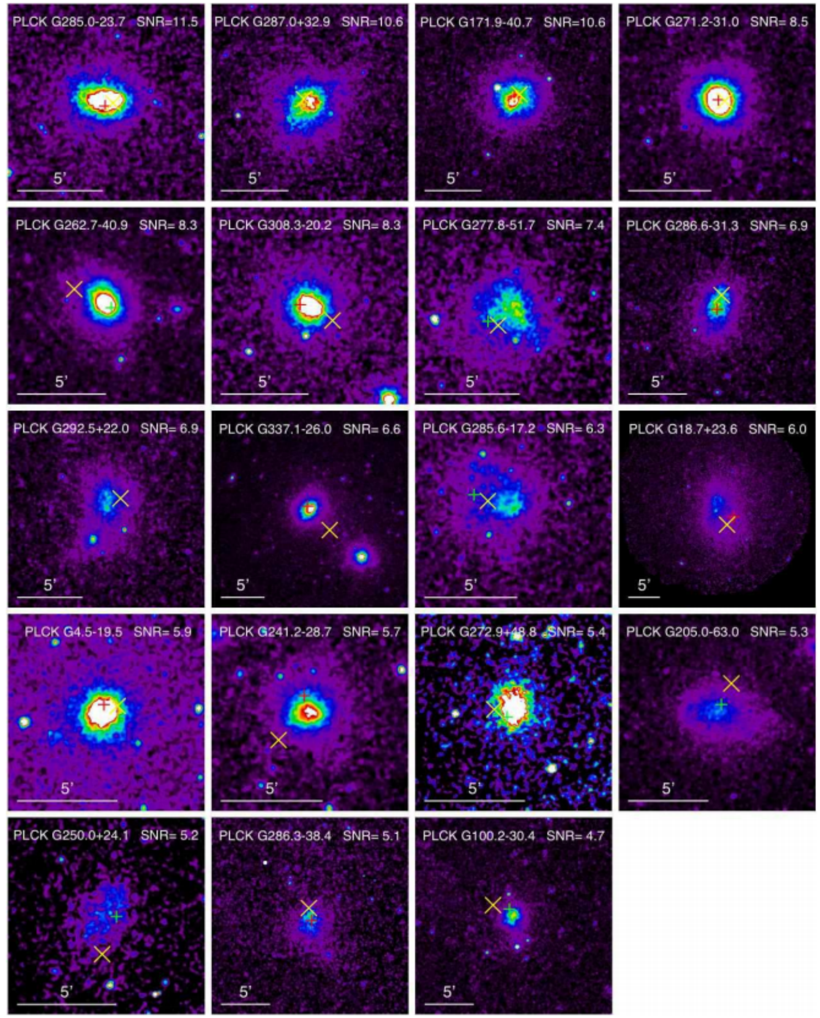

Fig. 5: *XMM-Newton* images of all confirmed cluster candidates, except for the two triple systems, in the [0.3–2] keV energy band. The observations of PLCK G272.9+48.8 and PLCK G250.0+24.1 suffer from high background that has only been crudely subtracted. Image sizes are $3\theta_{500}$ on a side, where θ_{500} is estimated from the M_{500}–Y_X relation (see Sec. 5.1). Images are corrected for surface brightness dimming with z, divided by the emissivity in the energy band, taking into account galactic absorption and instrument response, and scaled according to the self-similar model. The colour table is the same for all clusters, so that the images would be identical if clusters obeyed strict self-similarity. The majority of the objects show evidence for significant morphological disturbance. A yellow cross indicates the *Planck* position and a red/green plus sign the position of a *RASS*-BSC/FSC source.

21/25 success

2 super clusters

Planck Collaboration: *XMM-Newton* follow-up for validation of *Planck* cluster candidates

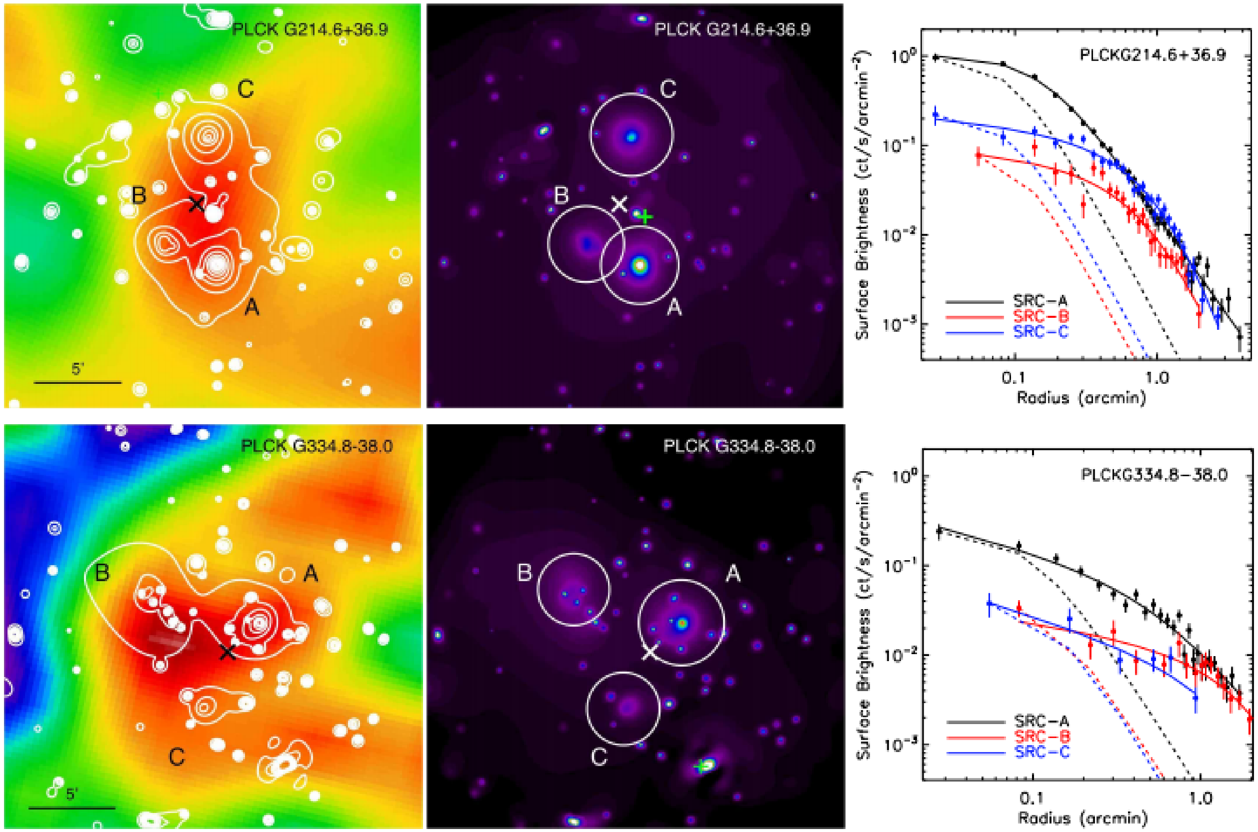

Fig. 12: The triple systems PLCK G214.6+37.0 (top) and PLCK G334.8-38.0 (bottom). The left panels show the *Planck* Y_{SZ} map (derived from an Internal Linear Combination method) with contours from the *XMM-Newton* wavelet filtered [0.3 – 2] keV image (middle panels) overlaid in white. The cross marks the position of the re-extraction centre for flux re-analysis. Extended components found in the *XMM-Newton* image are marked with letters (see text and Table 2). The circles in each *XMM-Newton* image denote the estimated R_{500} radius for each component. The right panels show the X–ray surface brightness profiles of the three components for each super cluster (points with uncertainties), and the best-fitting β-model (solid lines) compared to the profile of the Point Spread Function normalised at the central level (dashed lines).

No missing hot baryons

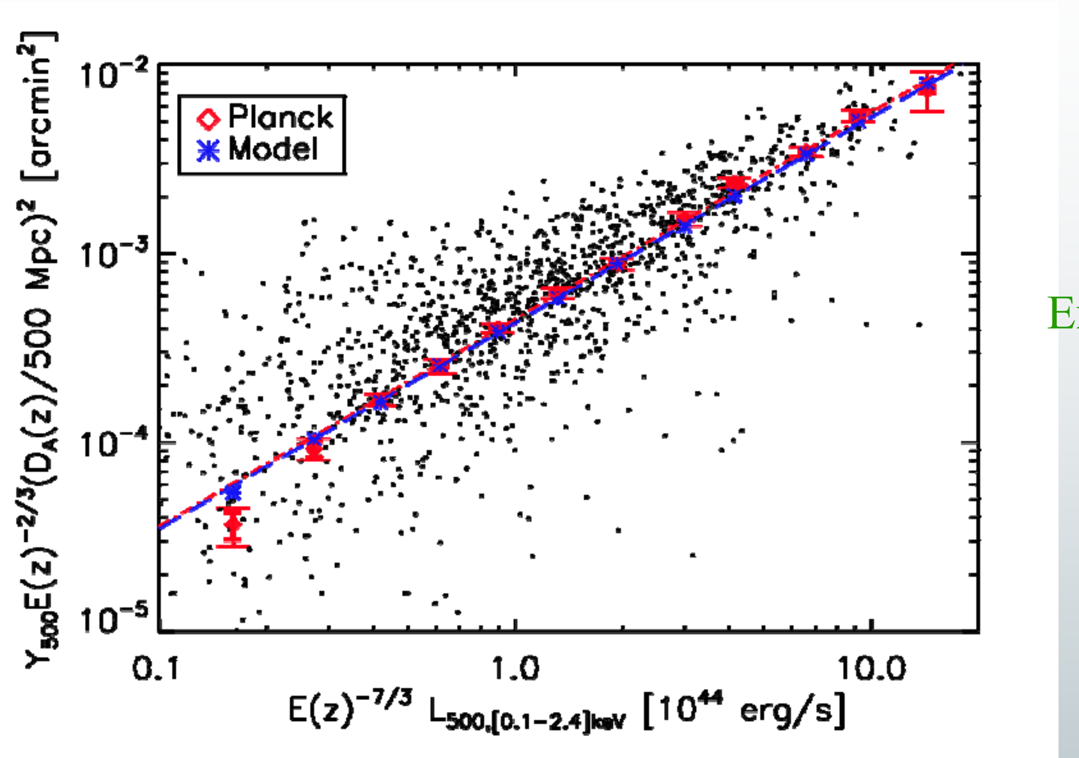

1882 X-ray selected clusters with homogenised L_{500}, z
MXCX (*Piffaretti et al 2010*)

Extraction and binning of Planck signal

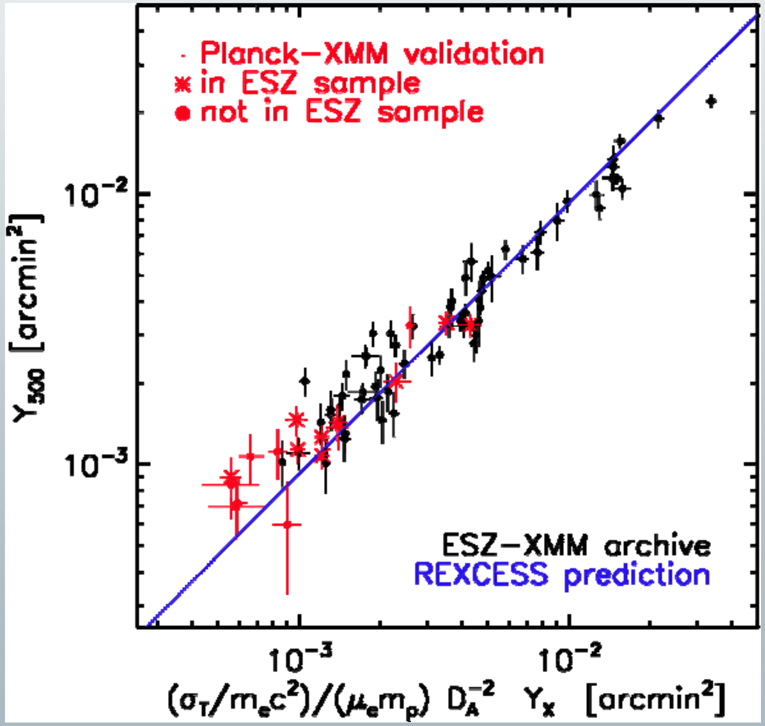

Compare SZ with X-ray expectations

Right: XMM follow-up

The Cosmic Infrared Background

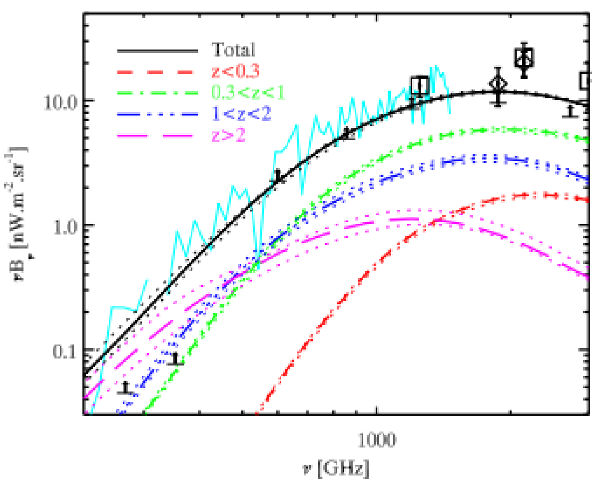

Figure 6. Contribution to the CIB per redshift slice, extracted from Béthermin et al. (2010c). The black solid line is the CIB spectrum predicted by the model. The contribution to the CIB from $0 < z < 0.3$, $0.3 < z < 1$, $1 < z < 2$ and $z > 2$ galaxies is given by the red short-dash, green dot-dash, blue three dot-dash and purple long-dashed lines, respectively. Lower limits coming from the stacking analysis at 100 μm, 160 μm (Berta et al. 2010), 250 μm, 350 μm, 500 μm (Marsden et al. 2009), 850 μm (Greve et al. 2009) and 1.1 mm (Scott et al. 2010) are shown as black arrows. The black diamonds give the Matsuura et al. (2010) absolute measurements with Akari. The black square the Lagache et al. (2000) absolute measurements with DIRBE/WHAM and the cyan line the Lagache et al. (2000) FIRAS measurement.

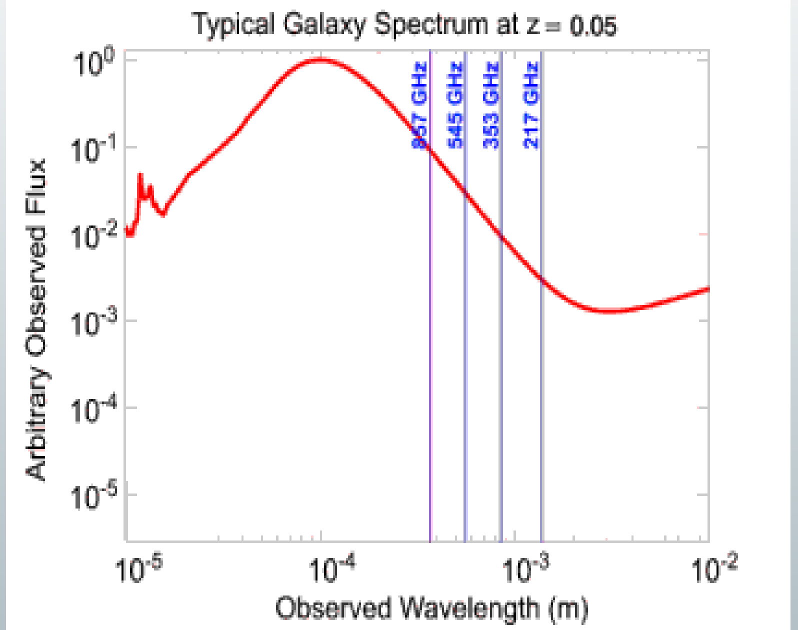

25 nW/m2/sr (CMB is 960)

The CIB anisotropies

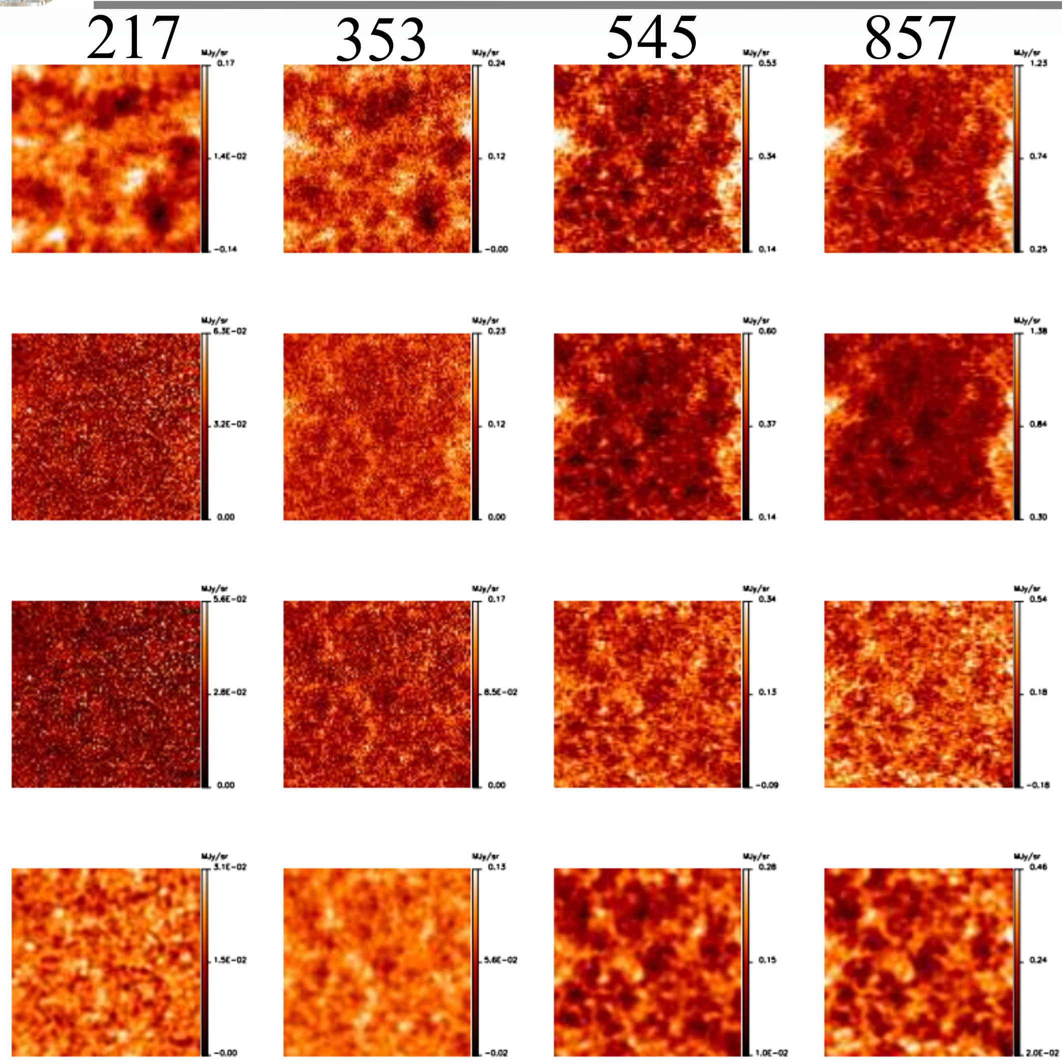

Figure 4. Maps of the 26 Sq. Deg. of the N1 field, from *left* to *right*: 217, 353, 545 and 857 GHz. From *top* to *bottom*: raw HFI maps; CMB- and ERCSC source-cleaned maps; residual maps (CMB-, sources-, and cirrus-cleaned); residual maps smoothed at 10′ to highlight the CIB anisotropies. The joint structures clearly visible (bottom row) correspond to the anisotropies of CIB. Residual point sources are also visible. They have fluxes lower than the fluxes of the ERCSC removed sources. They have no impact on our analysis.

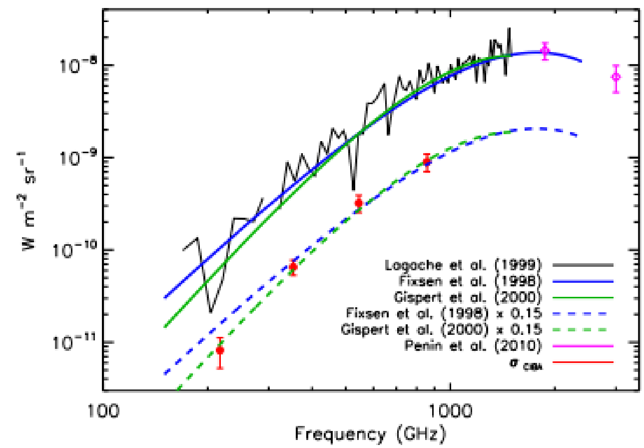

Figure 15. Comparison of the observed CIB mean and anisotropy SED. The CIB measurements are from Lagache et al. (1999) (*FIRAS* spectrum in black) and Penin et al. (2011) (*Spitzer* and *IRIS*, pink diamond data points). The green and blue continuous (dashed) lines are the CIB fits from Gispert et al. (2000) and Fixsen et al. (1998) (multiplied by 15%). The rms fluctuations of the CIB anisotropies, measured for $200 < \ell < 2000$, are shown with the red dots. Error bars include both statistical and systematic errors. This figure shows that the CIB anisotropy SED is steeper than the Fixsen et al. (1998) best fit but very close to the Gispert et al. (2000) best fit. We see no evidence for different CIB mean and anisotropy SED.

CIB Anistropy=15% CIB
0.02% for CMB

CIB comparison

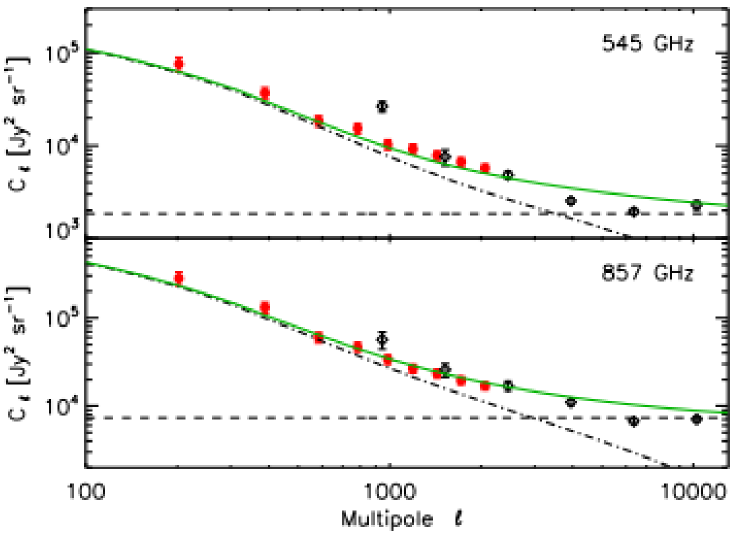

Figure 17. Comparison of BLAST and HFI measurements at 545 and 857 GHz. HFI data points are the red circles; BLAST data points are the black triangles. They have been color corrected for the comparison (the color has been computed using the CIB SED of Gispert et al. (2000), integrated through the BLAST and HFI bandpass filters). The dashed line is the BLAST shot noise (also color corrected). Also shown is the BLAST best fit clustering model (black dash-dotted line) and the total contribution (shot noise plus clustering; continuous green line). It provides a good fit to the *Planck* data.

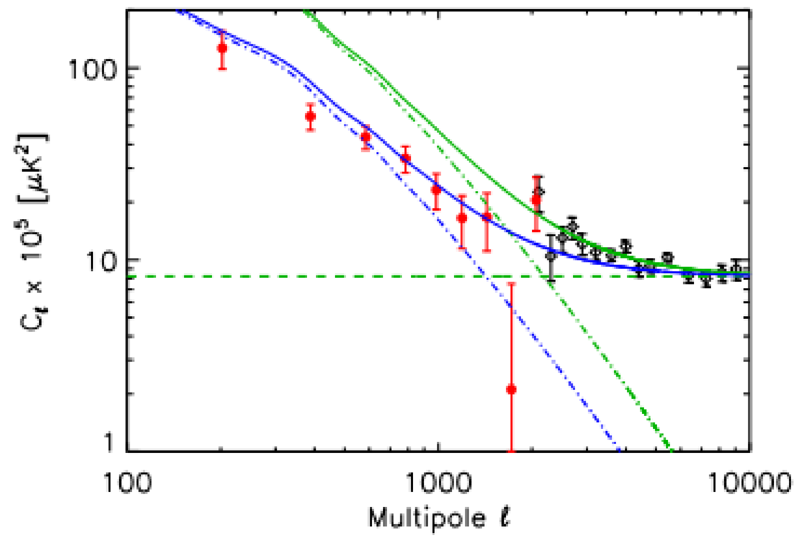

Figure 16. Comparison of SPT (Hall et al. 2010, dark triangles) and HFI measurements (red dots) at 217 GHz. The green dashed line corresponds to the SPT shot noise and the green dot-dashed line to the clustering model of Hall et al. (2010), the sum of the two being the continuous green line. The clustering model overpredicts by a factor $\simeq$ 2.4 the HFI power at ℓ = 800. When normalised by this factor (dash-dotted line) the clustering+shot noise (continuous line) now under-predicts the SPT data points, which may be the signature of non-linear contributions.

BLAST

SPT

Planck Goals

- Best precision on cosmological parameters
- Set the initial conditions for the large-scale structure formation
- Test the inflationary Big Bang paradigm with B modes
- Measure gravitational lensing and Non-Gaussianities
- Catalog of thousands of clusters of galaxies and CIB measurement
- Catalog of 10 000 clumps at the initial star forming stage
- Legacy: The (sub)millimetre and radio sky
- Serendipity! Rare objects

Agenda

- 14 may 2009 : launch
- 13 aout 2009 : start first survey (6 months= 95%)
- 13 february 2010: 2^{nd} survey
- 27 november 2010: end of nominal mission
- Jan 2011: Early Release Compact Source Cat.
- Feb 2011: 3^{rd} survey finished
- Jan 2012: end of HFI lifetime (about 5 surveys)
- End 2012: Cosmological results on nominal mission
- Jan 2013: Nominal mission data made public
- ~Jan 2014: Whole dataset public + final papers

The end

Additional Slides

WMAP / Planck

Couverture du ciel	Complète	Complète	
Système optique	2 télescopes dos-à-dos 1.4x1.6m Grégorien 90K	1 télescope de 1.5x1.8m Grégorien 50K	
Angle de balayage Par rapport à l'axe de rotation	±70°	85°	
Vitesse de rotation	0.5 tour/minute	1 tour/minute	
Modulation par précession	0.3 mHz précession	Non	
Détection	HEMT 90K	HEMT 20K	Bolomètres 0.1K
Polarisation (I, Q, U)	Oui	Oui	Oui sauf 545/857GHz
Principe de détection	Ciel/Ciel pseudo Corrélation différentielle	Ciel/Référence 4K différentielle	Modulation carrée Alternative
Étalonnage primaire	Dipôle CMB	Dipole CMB	
Mesure du lobe	Jupiter	Planètes (Mars, Jupiter, Saturne, Uranus, Neptune)	
Refroidissement	Passif	Passif + H_2 J-T (20K) + He J-T (4K)	
			He^3+He^4 J-T(1.6K) + He^3/He^4 open cycle dilution (0.1K)
Contrôle d'attitude	Contrôle 3-axes, 3 roues, gyros Senseur Stellaire et Solaire,	Contrôle par rotation, Thrusters et Senseur Stellaire et Solaire,	
Puissance	419 W	2000-1800 W	
Masse	840 kg	1900 kg	
Lancement	Delta II 30 Juin 2001	Ariane 5 ECA (avec HSO) 14 mai 2009	
Trajectoire	3 boucles avec la lune 3 mois	Direct vers L2, 45 jours	
Durée requise	3 mois+2 ans	3 mois + 14 mois	

WMAP basics

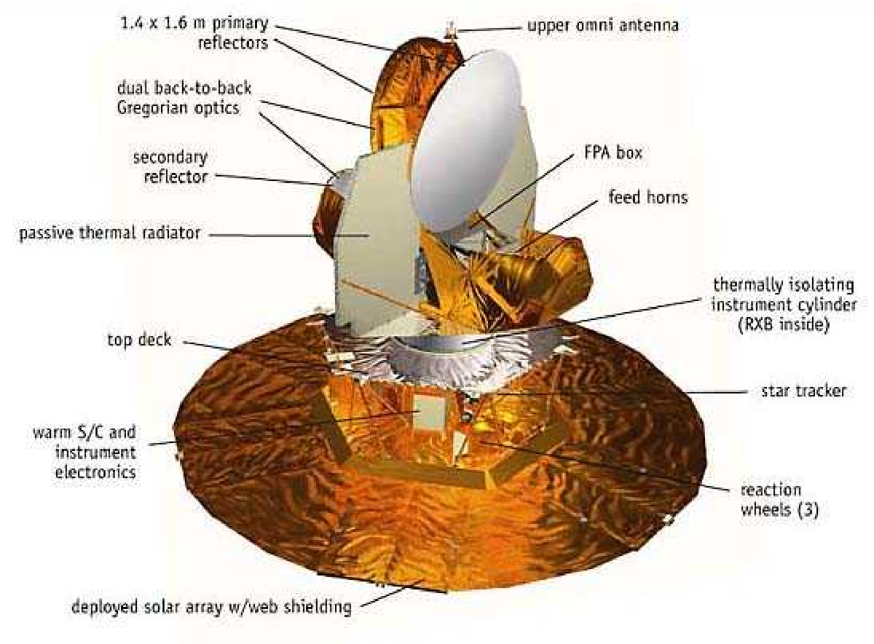

1.4 x 1.6 m primary reflectors
upper omni antenna
dual back-to-back Gregorian optics
secondary reflector
FPA box
feed horns
passive thermal radiator
thermally isolating instrument cylinder (RXB inside)
top deck
star tracker
warm S/C and instrument electronics
reaction wheels (3)
deployed solar array w/web shielding

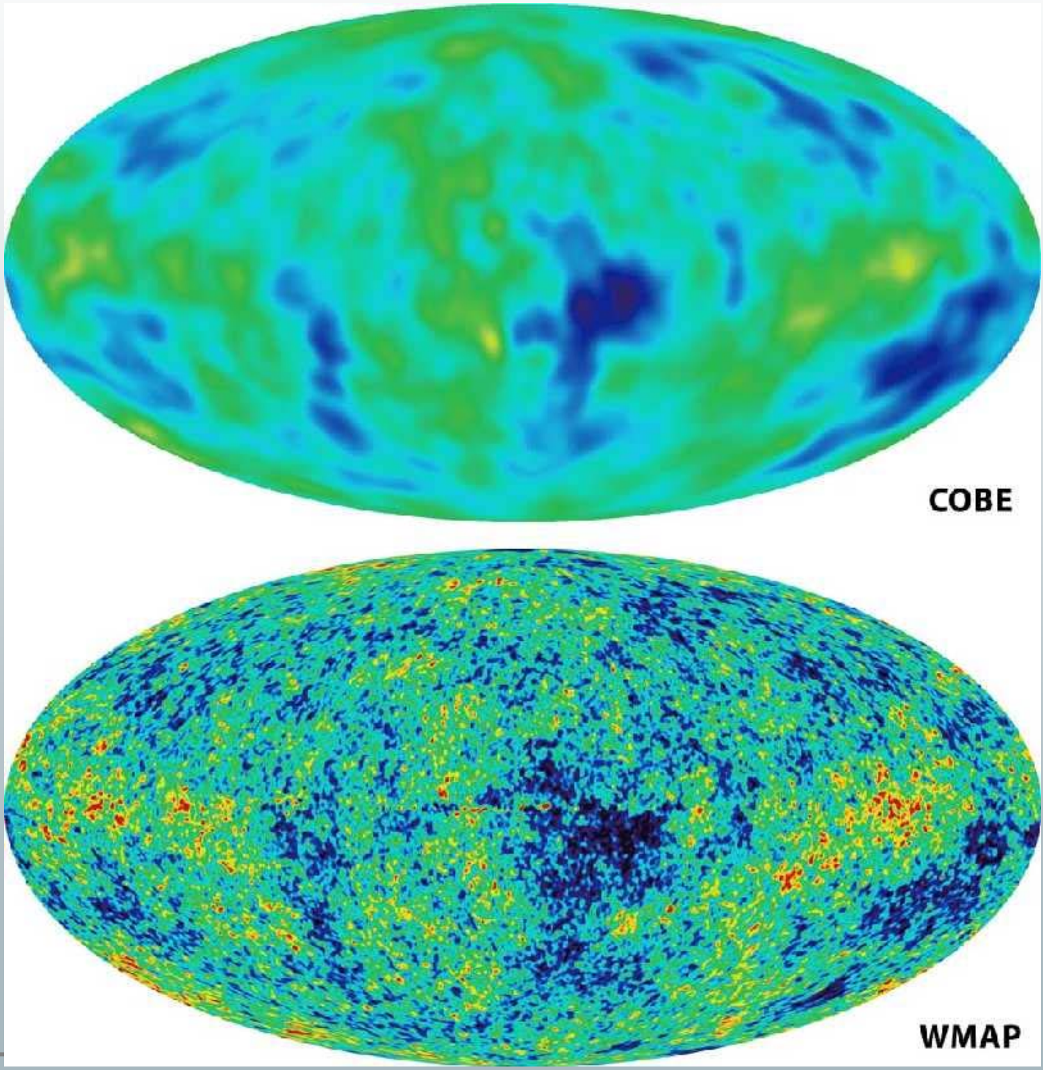

COBE
WMAP